

# **The O-GlcNAc transferase OGT is a conserved and essential regulator of the cellular and organismal response to hypertonic stress**

Sarel J. Urso<sup>1,4</sup>, Marcella Comly<sup>2</sup>, John A. Hanover<sup>2</sup> and Todd Lamitina<sup>\*</sup>, <sup>1,3,4</sup>

<sup>1</sup>Graduate Program in Cell Biology and Molecular Physiology, University of Pittsburgh School of Medicine, Pittsburgh, PA, 15261, USA

<sup>2</sup>Laboratory of Cellular and Molecular Biology, National Institute of Diabetes and Digestive and Kidney Diseases, National Institute of Health, Bethesda, MD, 20892, USA

<sup>3</sup>Division of Child Neurology, Department of Pediatrics, Children's Hospital of Pittsburgh, Pittsburgh, PA, 15224, USA

<sup>4</sup>Department of Cell Biology, University of Pittsburgh School of Medicine, Pittsburgh, PA, 15261, USA

\*Address correspondence to Todd Lamitina, Ph.D., Children's Hospital of Pittsburgh of the University of Pittsburgh Medical Center, Departments of Pediatrics and Cell Biology, 4401 Penn Avenue, Rangos 7122, Pittsburgh, PA 15224, phone - (412) 692-9437; fax – (412) 641-1844; email - stl52@pitt.edu

**Short Title:** Hypertonic stress response requires OGT

## Abstract

The conserved O-GlcNAc transferase OGT O-GlcNAcylates serine and threonine residues of intracellular proteins to regulate their function. OGT is required for viability in mammalian cells, but its specific roles in cellular physiology are poorly understood. Here we describe a conserved requirement for OGT in an essential aspect of cell physiology: the hypertonic stress response. Through a forward genetic screen in *Caenorhabditis elegans*, we discovered OGT is acutely required for osmoprotective protein expression and adaptation to hypertonic stress. Gene expression analysis shows that *ogt-1* functions through a post-transcriptional mechanism. Human OGT partially rescues the *C. elegans* phenotypes, suggesting that the osmoregulatory functions of OGT are ancient. Intriguingly, mutations that ablate O-GlcNAcylation activity in either human or *C. elegans* OGT rescue the hypertonic stress response phenotype. Our findings are among the first to demonstrate a specific physiological role for OGT at the organismal level and demonstrate that OGT engages in important molecular functions outside of its well described roles in post-translational O-GlcNAcylation of intracellular proteins.

**Keywords:** cellular stress, *Caenorhabditis elegans*, osmotic stress, osmoprotective gene expression, cell volume, genetic screen, whole genome resequencing, signaling, post-transcriptional gene expression

## Author Summary

The ability to sense and adapt to changes in the environment is an essential feature of cellular life. Changes in environmental salt and water concentrations can rapidly cause cell volume swelling or shrinkage and, if left unchecked, will lead to cell and organismal death. All organisms have developed similar physiological strategies for maintaining cell volume. However, the molecular mechanisms that control these physiological outputs are not well understood in animals. Using unbiased genetic screening in *C. elegans*, we discovered that a highly conserved enzyme called O-GlcNAc transferase (OGT) is essential for regulating physiological responses to increased environmental solute levels. A human form of OGT can functionally substitute for worm OGT, showing that this role is conserved across evolution. Surprisingly, the only known enzymatic activity of OGT was not required for this role, suggesting this enzyme has important undescribed molecular functions. Our studies reveal a new animal-specific role for OGT in the response to osmotic stress and show that *C. elegans* is an important model for defining the conserved molecular mechanisms that respond to alterations in cell volume.

## Introduction

Cells must adapt to perturbations in extracellular osmolarity to maintain cell volume, membrane tension, and turgor pressure (1). Hypertonic stress leads to loss of cell volume, increased intracellular ionic strength, and protein dyshomeostasis. Failure to initiate protective mechanisms against these perturbations leads to cell death (2). Hypertonicity contributes to several pathophysiological conditions and is also a feature of normal physiological states such as those that exist in the kidney and thymus (3, 4). Cells in these tissues can survive in hypertonic conditions because of evolutionarily conserved adaptive mechanisms.

Cells adapt to hypertonic stress primarily through the cytosolic accumulation of small uncharged molecules called organic osmolytes (5). These organic osmolytes track extracellular osmolarity to maintain intracellular water content and cell volume. Additionally, through their chemical chaperone activity, osmolytes can also oppose the protein misfolding and aggregation that is a consequence of hypertonic stress (6). Cells can accumulate hundreds of millimolar concentrations of organic osmolytes within hours of exposure to hypertonic stress. Osmolyte accumulation occurs either through the activity of specialized osmolyte transporters or osmolyte biosynthetic enzymes. In all cases, these transporters or biosynthesis enzymes are upregulated at the transcriptional and translational level by hypertonic stress (7). The molecular identity of osmolyte transporters and biosynthetic enzymes utilized to accumulate osmolytes is highly variable between organisms and even between cells within the same organism. This is because there is a significant chemical diversity among osmolytes through phylogeny due to metabolic, nutritional, and ecological limitations (5).

One chemical class of osmolytes is carbohydrate polyols such as sorbitol and glycerol. During hypertonic stress, mammalian kidney epithelial cells upregulate the

enzyme aldose reductase to synthesize sorbitol from glucose (8). Likewise, *C. elegans* upregulates the biosynthetic enzyme glycerol-3-phosphate dehydrogenase (*gpdh-1*) to synthesize glycerol from glucose during exposure to hypertonic stress (9, 10). Both sorbitol and glycerol accumulation provide osmoprotective effects, such as increased cellular volume, decreased intracellular ionic strength, and improved protein homeostasis. At the organismal level in *C. elegans*, decreased glycerol biosynthesis is associated with decreased fecundity and growth under hypertonic conditions (10). In addition to osmolyte accumulation genes, hundreds of other genes are also upregulated during hypertonic stress (11). While some of the transcriptional mechanisms leading to upregulation of these genes are known, post-transcriptional regulatory mechanisms are poorly understood (11, 12).

The O-GlcNAc transferase OGT is the sole protein that adds the single ring sugar, O-GlcNAc, to serine and threonine residues of hundreds of intracellular proteins to modify their function, stability, and localization. The O-GlcNAcase OGA is the sole enzyme that removes O-GlcNAc from proteins. OGT and OGA together regulate cellular O-GlcNAc homeostasis, which is important to a variety of cellular processes including metabolism, stress responses, and proteostasis (13, 14). Importantly, O-GlcNAc catalytic activity is not the only function of OGT. OGT proteolytically cleaves and activates the mammalian host cell factor C1 (HCF-1) (15, 16). OGT also has non-catalytic scaffolding functions in cell adhesion and neuronal synaptic transmission (17, 18).

All metazoans express a single *ogt* gene, which is absent from yeast (19, 20). Knockout of OGT in most metazoans is lethal at either the single cell or developmental level. The notable exception to this is *C. elegans*, where *ogt-1* null mutants are viable under standard cultivation conditions. Here, we show that *C. elegans ogt-1* mutants are

non-viable under a specific physiological condition, hypertonic stress. Through an unbiased screen, we identified *ogt-1* as being required for expression of the osmosensitive *gpdh-1p::GFP* reporter. We found that under hypertonic stress conditions, *ogt-1* is required for accumulation of GPDH-1 protein, but not *gpdh-1* mRNA. Additionally, *ogt-1* mutants are unable to grow and reproduce following exposure to mild hypertonic environments. Finally, we demonstrate that expression of human OGT can rescue the *C. elegans* hypertonic stress phenotype. The ability of either human or *C. elegans* OGT to rescue is independent of O-GlcNAcylation catalytic activity. These results demonstrate for the first time a specific role for OGT in the essential process of osmoregulation and suggest that this function is conserved across >700 million years of evolution.

## Results

### **An unbiased forward genetic screen for ‘no induction of osmolyte biosynthesis gene expression’ (Nio) mutants identifies the conserved O-GlcNAc transferase *ogt-1***

In *C. elegans*, hypertonic stress rapidly and specifically upregulates expression of the osmolyte biosynthesis gene *gpdh-1*, which we visualized with a *gpdh-1p::GFP* transcriptional reporter (10, 11). To optimize this reporter for genetic screening, we added a *col-12p::dsRed* reporter, whose expression is not affected by hypertonic stress and serves as an internal control for non-specific effects on gene expression (21). This dual reporter strain (*drIs4*) expresses only dsRed under isotonic conditions and both dsRed and GFP under hypertonic conditions, with very few animals exhibiting an intermediate phenotype (Figure 1A - C). A *gpdh-1p::GPDH-1::GFP* translational reporter (*kbls6*) is also upregulated by hypertonic stress, but exhibits more variability than the *drIs4* transcriptional reporter (Figure 1D - F).

Taking advantage of the binary nature of GFP activation by hypertonic stress in the *drIs4* strain, we designed an unbiased F2 forward genetic screen for mutants that fail to activate GFP expression during hypertonic stress, but exhibit no effects on RFP (‘no induction of osmolyte biosynthesis gene expression’) mutants; Figure 2A). From this screen of ~120,000 haploid genomes, we identified two recessive alleles, *dr15* and *dr20*, that genetically fail to complement each other. Whole genome sequencing and bioinformatics revealed that each allele contained a distinct nonsense mutation in the gene encoding the O-GlcNAc transferase *ogt-1* (Table S1 - 3, Figure 2B). Two independently isolated *ogt-1* deletion alleles, *ok430* and *ok1474*, as well as wild type worms exposed to *ogt-1(RNAi)* also exhibited a Nio phenotype, and *ok430* and *ok1474*

failed to complement the *dr15* and *dr20* alleles. (Figure 2B - D, S1A - B, Table S2).

CRISPR reversion of the *dr20* Q600STOP mutation back to wild type, as well as transgenic overexpression of wild type *ogt-1* in the *dr20* mutant, was sufficient to rescue the *ogt-1* Nio phenotype, indicating that other ENU induced mutations in the background do not contribute to the Nio phenotype (Figure 2E and S1C). Finally, we found that knock down of *ogt-1* during post-developmental stages with *ogt-1(RNAi)* was sufficient to cause a Nio phenotype, suggesting that OGT-1 is not required for the establishment of developmental structures necessary for responding to hypertonic stress (Figure 2F). The function of *ogt-1* in the response to hypertonic stress is specific because inhibition of *ogt-1* did not affect either heat shock or endoplasmic reticulum stress inducible reporter expression (Figure S2). In conclusion, these results suggest that *ogt-1* is specifically and acutely required for hypertonic stress-induced upregulation of *gpdh-1* expression.

### **OGT-1 is required for osmosensitive protein expression, but not osmosensitive transcription.**

Since *ogt-1* is required for induction of the *gpdh-1p::GFP* transgenic reporter by hypertonic stress, we hypothesized that endogenous osmosensitive mRNAs would not be upregulated in an *ogt-1* mutant. To test this, we used qPCR to measure the expression levels of several previously described mRNAs that are induced by osmotic stress (11). Surprisingly, we found that osmosensitive mRNA expression was still upregulated in *ogt-1* mutants (Figure 3A and S3A). Consistent with this, we also observed that GFP mRNA derived from the *gpdh-1p::GFP* reporter was upregulated by hypertonic stress in *ogt-1* mutants even though GFP protein levels were strongly reduced (Figure 3B, 2D, S1A). These data unexpectedly suggest that OGT-1 regulates osmosensitive gene expression at a post-transcriptional level.

To further examine if OGT-1 affects the coupling between hypertonic stress induced mRNA and protein expression, we measured GPDH-1 protein levels in *ogt-1* mutants. As we observed for the *gpdh-1p::GFP* transcriptional reporter, *ogt-1* mutants failed to induce the GPDH-1::GFP protein in response to hypertonic stress (Figure 3C and S3B). However, the mRNA from this translational reporter was still induced to wild type levels (Figure 3D). Importantly the requirement for *ogt-1* in the hypertonic stress response is not transgene dependent because *ogt-1* is also required for the hypertonic induction of CRISPR/Cas9 engineered GPDH-1::GFP fusion protein, which we confirmed to be functional (Figure 3E and S4C). In conclusion, these results suggest that OGT-1 functions downstream of osmosensitive mRNA upregulation, but upstream of osmosensitive protein expression.

### **Physiological and genetic adaptation to hypertonic stress requires *ogt-1***

*C. elegans* upregulate osmosensitive genes, including *gpdh-1*, to survive and adapt to hypertonic challenges. We found that loss of *ogt-1* had no effect on acute survival during hypertonic stress (Figure S4A) (10). However, loss of *ogt-1* blocked the ability of animals to adapt, grow, and reproduce under mild hypertonic stress (Figure 4A and S4B). This adaptation phenotype was rescued by CRISPR reversion of the *dr20* Q600STOP mutation to wild type (Figure S4C). Interestingly, the adaptation phenotype of *ogt-1* mutants must extend beyond its effects on *gpdh-1*, since the adaptation phenotype of a *gpdh-1* presumptive null mutant is not as severe as that observed in an *ogt-1* mutant (Figure 4A).

In addition to physiological exposures, adaptation to hypertonic stress can also be induced genetically via loss of function mutations in several hypodermis expressed secreted extracellular matrix (ECM) proteins (11, 12). These mutants exhibit maximal induction of *gpdh-1* mRNA and accumulation of glycerol. As a result these mutants are constitutively adapted to survive normally lethal levels of hypertonic stress (11, 12). To test if *ogt-1* is required for genetic adaptation to hypertonic stress, we introduced an *ogt-1* mutation into *osm-8(dr9)* or *osm-11(n1604)* mutants. Both *osm-8* and *osm-11* mutants exhibit constitutively elevated *gpdh-1p::GFP* expression under isotonic conditions. However, *gpdh-1p::GFP* levels were significantly reduced in *osm-8;ogt-1* and *osm-11;ogt-1* double mutants (Figure 4B and S4D). Consistent with this observation, the ability of *osm-8* mutants to survive a lethal hypertonic stress was suppressed in the *osm-8;ogt-1* double mutants (Figure 4C) (12). These data suggest that *ogt-1* is required for both physiological and genetic adaptation to hypertonic stress caused by loss of the ECM proteins OSM-8 and OSM-11.

### **Non-canonical activity of *ogt-1* in the hypodermis regulates *gpdh-1* induction by hypertonic stress through a functionally conserved mechanism.**

In *C. elegans*, functional endogenously GFP tagged *ogt-1* is ubiquitously expressed in the nucleus, consistent with previous observations (Figure S4C and S5A) (22).

Therefore, we used tissue specific promoters to test which tissues require *ogt-1* expression for *gpdh-1* induction by hypertonic stress. The expression of *ogt-1* from either its native promoter or a hypodermal specific promoter was sufficient to rescue *gpdh-1* induction by hypertonic stress in *ogt-1* LOF mutants. However, expression of *ogt-1* in intestine, muscle, or neurons did not rescue (Figure 5A - B). Since *gpdh-1* is

induced by hypertonic stress in the hypodermis, these results suggest that *ogt-1* acts cell autonomously in the hypoderm to regulate osmosensitive protein expression.

Given that *C. elegans* OGT-1 is highly conserved with human OGT (Fig. 2B), we asked if human OGT could functionally replace *C. elegans* OGT-1 in the hypertonic stress response. Overexpression of a human OGT cDNA from the native *C. elegans ogt-1* promoter partially rescued *gpdh-1p::GFP* induction by hypertonic stress in an *ogt-1* LOF mutant (Figure 5C - D). Unexpectedly, catalytically dead human OGT (OGT H498A) rescued *gpdh-1p::GFP* induction by hypertonic stress in an *ogt-1(dr20)* LOF mutant to the same extent as wild type human OGT (Figure 5C - 5D) (23, 24). To further test the requirement for OGT-1 O-GlcNAcylation in the hypertonic stress, we CRISPR engineered catalytically inactive mutations into the endogenous *C. elegans ogt-1* locus (H612A and K957M, equivalent to human H498A and K842M) (18, 24). Surprisingly, only the K957M mutation suppressed O-GlcNAcylation activity completely. The H612A mutation reduced O-GlcNAcylation but did not eliminate it. However, neither the K957M nor the H612A mutation altered OGT-1 protein levels or nuclear localization (Figure S5). In agreement with the results from the catalytically dead human OGT, *C. elegans* expressing catalytically impaired alleles of endogenous *ogt-1* induced *gpdh-1p::GFP* during hypertonic stress and had normal adaptation to hypertonic stress (Figure 5E - G). In conclusion, a non-catalytic function of OGT-1 in the hypodermis is required for osmosensitive protein induction by hypertonic stress. Importantly, this non-catalytic stress-responsive function is conserved from *C. elegans* to human OGT.

## Discussion

Through an unbiased forward genetic screen for mutants that disrupt osmosensitive expression of a *gpdh-1::GFP* reporter in *C. elegans*, we identified multiple

alleles of the O-GlcNAc transferase OGT-1. This *ogt-1* phenotype is specific to hypertonic stress since *ogt-1* is not required for upregulation of other stress responsive reporters. *ogt-1* likely functions as a key signaling component of the hypertonic stress response, since post-developmental knockdown of *ogt-1* was sufficient to produce the Nio phenotype. *ogt-1*-dependent signaling in the hypertonic stress response appears to occur primarily in the hypodermis, a known osmosensitive tissue in *C. elegans* (10, 12). The mechanism by which *ogt-1* regulates hypertonicity induced gene expression was unexpected. *ogt-1* mutants exhibited normal hypertonicity induced upregulation of stress response mRNAs. However, levels of the encoded proteins were significantly reduced, suggesting *ogt-1* acts via a post-transcriptional mechanism(s). *ogt-1* mutants are completely unable to adapt and reproduce in hypertonic environments and this correlates with an inability of *ogt-1* mutants to properly upregulate the translation of osmoprotective proteins such as *gpdh-1*. Intriguingly, we demonstrate that the function of *ogt-1* in the hypertonic stress response does not require O-GlcNAcylation catalytic activity. Both wild type and catalytically inactive human OGT can rescue the *C. elegans* *ogt-1* Nio phenotypes, suggesting that this non-catalytic function is also conserved with humans (Figure 6).

*C. elegans* is the primary genetic model system for studies of *ogt-1* because it is the only organism in which loss of *ogt-1* is viable (25, 26). This has allowed many previous studies to parse the roles of *ogt-1* in lifespan, metabolism, innate immunity, behavior, neuron function, stress responses, cell fate, and autophagy (18, 22, 25, 27-36). Importantly, most of these studies utilized global *ogt-1* knockdown, which eliminates both O-GlcNAcylation-dependent and –independent functions of *ogt-1*. The missense alleles generated here will provide powerful tools for differentiating between these functions.

Our studies reveal a critical and previously unappreciated condition-specific role of OGT-1 in adaptation to hypertonic stress. This phenotype is completely penetrant and one of the strongest *ogt-1* phenotypes described to date. Although their ability to survive acute hypertonic stress is unaffected, *ogt-1* mutants are unable to adapt and reproduce following extremely mild shifts in extracellular osmolarity (250 mM NaCl). Such conditions have minimal effects on the ability of wild type animals to adapt and reproduce (10). This suggests a critical physiological role of *ogt-1* in the ability of *C. elegans* to survive in the wild, since worms are continuously exposed to fluctuating environmental salinity in their native ecosystems (37). Given that both *C. elegans* and human OGT are able to rescue the Nio phenotype of *ogt-1* mutants in *C. elegans*, we speculate that OGT plays an ancient and conserved physiological function in response to environmental and physiological perturbations in osmotic homeostasis.

In mammals, OGT is essential for cell division, a physiological process that involves tight regulation of cell volume (26, 38-40). Therefore, we speculate that OGT may be required for mammalian cell division for the same reason it is essential for adaptation to hypertonic stress in *C. elegans*: it plays a critical role in cell volume regulation. One reason mammalian cells may be unable to divide without OGT is because they cannot properly regulate cell volume during cell division. In *C. elegans*, unlike in mammals, *ogt-1* is not an essential gene. We hypothesize that the osmotic homogeneity of standard *C. elegans* lab culture conditions allows *ogt-1* mutants to survive and propagate normally. However, under hypertonic conditions, *ogt-1* becomes an essential gene in *C. elegans*, like it is in humans. It will be interesting to explore the roles and requirements of OGT in cell volume regulation in mammalian cells and tissues.

Knockout of OGT in mammalian cells leads to a rapid loss in cellular viability (26). This phenotype is largely thought to be due to loss of O-GlcNAcylation activity. However, data from human cells suggest that O-GlcNAcylation activity may not be the essential function of OGT. For example, exposure of mammalian cells to the O-GlcNAc inhibitor Ac<sub>4</sub>-5SGlcNAc largely blocks O-GlcNAcylation, but cellular viability and division are unaffected (41). Additionally, cells and humans carrying inherited catalytic point mutations in OGT associated with intellectual disability are viable (42). Our data show that the role of OGT-1 in the *C. elegans* hypertonic stress response is also independent of catalytic activity. Such catalytically-independent roles of OGT-1 have also been described in the context of synaptic regulation and cell adhesion (17, 18). If the evolutionarily critical role of OGT in mammalian cells is related to its ability to regulate cell volume, our data suggest that such functions are independent of O-GlcNAcylation activity. These non-catalytic functions of OGT and the protein domains that regulate these functions are largely unexplored. The *C. elegans* Nio phenotype may provide a powerful genetic system for identifying new functional domains important for OGT function via targeted and unbiased genetic screening strategies.

Cell volume regulation during environmental stress requires upregulation of osmoprotective proteins, including those that regulate osmolyte accumulation. In almost all cases, these genes are upregulated at the transcriptional level (11). Our findings are the first evidence that this pathway is also under post-transcriptional control. OGT-1 is required for the accumulation of GPDH-1 protein during hypertonic stress, but not for the upregulation of *gpdh-1* mRNA. Interestingly, this is not a complete elimination of GPDH-1 protein induction and even if it were, *gpdh-1* null mutants still retain significant hypertonic adaptation potential, whereas *ogt-1* mutants are completely adaptation deficient. These results suggest that OGT-1 regulation of the hypertonic stress

response is likely to extend beyond its effects on post-transcriptional GPDH-1 induction.

The nature of these additional targets and/or mechanisms is currently unknown.

The regulation of stress responsive gene expression by OGT is not a new paradigm. Previous data has shown that it plays both a transcriptional and post-transcriptional role in stress response gene expression. For example, OGT-1 O-GlcNAcyates the oxidative stress responsive transcription factor SKN-1 to facilitate upregulation of antioxidant gene transcription (32). On the other hand, OGT regulates UPR<sup>ER</sup> and HSR gene expression post-transcriptionally by O-GlcNAcyating translation initiation factors to selectively facilitate translation of stress induced mRNAs (43, 44). Importantly, all of the previously described roles of OGT in stress responses require O-GlcNAcylation. While our data suggests that OGT-1 also functions in the hypertonic stress response through a post-transcriptional mechanism, this mechanism is fundamentally different from that of the oxidative, HSR, and UPR<sup>ER</sup> stress responses because it does not require OGT O-GlcNAcylation activity (43, 44). Further mechanistic studies are needed to define the O-GlcNAcylation-independent downstream targets and mechanisms of OGT-1 required for osmoprotective protein expression.

Since the discovery of OGT, *C. elegans* have been an important tool for characterizing the role of OGT in cell signaling because they are the only organism in which genetic loss of OGT generates viable cells and organisms (20, 25). However, it is still unknown why *ogt-1* null *C. elegans*, in contrast to every other metazoan, are viable (45). One possibility is that the evolutionarily conserved role of *ogt-1* in cell volume regulation during hypertonic stress contributes to the essential role of OGT in all metazoans, including *C. elegans*. However, several key questions about the osmoprotective nature of OGT still remain. First, while canonical OGT-1-dependent O-GlcNAcylation is dispensable for the hypertonic stress response, it remains unclear

which functions of *ogt-1* are important to this physiological process. Although OGT-1 can also catalyze a unique type of proteolysis event, this activity is not thought to occur in *C. elegans* (46). Regardless, the K957M mutation also eliminates the known proteolytic activity of *ogt-1*, suggesting that this function is also not required in the hypertonic stress response (24). Future studies, utilizing both targeted *ogt-1* deletion alleles and unbiased genetic screens for new *ogt-1* missense mutations with a Nio phenotype, should help resolve this question. Second, the precise post-transcriptional mechanism under OGT-1-dependent control remains unknown. Such mechanisms could include mRNA cleavage and polyadenylation site usage, mRNA nuclear export, selective interactions between ribosomes and stress-induced mRNAs, or regulated proteolysis of stress-induced proteins such as GPDH-1. While most of these potential mechanisms await testing, we find that inhibition of either autophagic or proteasome-mediated proteolysis does not appear to be involved (Figure S6). Finally, it remains unclear which genes *ogt-1* coordinates with to regulate hypertonic stress signaling. Future studies analyzing new Nio mutants should shed light on these interactions.

In conclusion, our unbiased genetic screening approaches in *C. elegans* have revealed a previously unappreciated requirement for non-canonical OGT signaling in a critical and conserved aspect of cell physiology. The primary function of OGT has long been assumed to be due to its catalytic O-GlcNAcylation activity. However, as we and others have shown, OGT also has critical and conserved non-catalytic functions that warrant further study (17, 18). It is vital that future studies involving OGT utilize point mutants that differentiate canonical from non-canonical functions rather than OGT knockouts, which ablate both. As our studies have shown, such approaches could reveal new roles for this key protein in unexpected aspects of cell physiology.



# Materials and methods

## C. elegans strains and culture

Strains were cultured on standard NGM media with *E.coli* OP50 bacteria at 20°C unless otherwise noted. The following strains were used; N2 Bristol WT, OG119 *drls4* [*gpdh-1p::GFP*; *col-12p::dsRed2*], VP223 *kbls6* [*gpdh-1p::gpdh-1-GFP*], OG971 *ogt-1(dr15);drls4*, OG969 *ogt-1(dr20);drls4*, OG1034 *ogt-1(ok430);drls4*, OG1035 *ogt-1(ok1474);drls4*, OG1066 *ogt-1(dr20 dr36);drls4*, OG1064 *ogt-1(dr34);unc-119(ed3);kbls6*, OG1115 *gpdh-1(dr81)* [*gpdh1::GFP*], OG1123 *gpdh-1(dr81);ogt-1(dr84)*, RB1373 *gpdh-1(ok1558)*, OG1048 *osm-8(dr9);unc-4(e120);drls4*, OG1049 *osm-8(dr9);unc-4(e120);ogt-1(dr20);drls4*, OG1111 *ogt-1(dr20);drls4;drEx468* [*ogt-1p::ogt-1cDNA::ogt-13'utr*; *rol-6(su1006)*], OG1119 *ogt-1(dr20);drls4;drEx469* [*dpy-7p::ogt-1cDNA::ogt-13'utr*; *rol-6(su1006)*], OG1120 *ogt-1(dr20);drls4;drEx470* [*nhx-2p::ogt-1cDNA::ogt-13'utr*; *rol-6(su1006)*], OG1121 *ogt-1(dr20);drls4;drEx471* [*myo-2p::ogt-1cDNA::ogt-13'utr*; *rol-6(su1006)*], OG1122 *ogt-1(dr20);drls4;drEx472* [*rab-3p::ogt-1cDNA::ogt-13'utr*; *rol-6(su1006)*], OG1125 *ogt-1(dr20);drls4;drEx473* [*ogt-1p::human OGT isoform 1cDNA::ogt-13'utr*; *rol-6(su1006)*], OG1126 *ogt-1(dr20);drls4;drEx474* [*ogt-1p::human OGT isoform 1 H498AcDNA::ogt-13'utr*; *rol-6(su1006)*], OG1046 *ogt-1(dr20);drls4;drEx465* [*ogt-1p::ogt-1 genomic*], TJ375 *gpls1* [*hsp16.2p::GFP*], SJ4005 *zcls4* [*hsp4::GFP*] V, OG1081 *ogt-1(dr50);zcls4*, MT3643 *osm-11(n1604)*, OG1083 *ogt-1(dr52);osm-11(n1604)*, OG1135 *ogt-1(dr86);drls4*, OG1140 *ogt-1(dr90);drls4*, OG1124 *ogt-1(dr84)* [*ogt-1::GFP*], OG1139 *ogt-1(dr84);ogt-1(dr89)*, OG1141 *ogt-1(dr84);ogt-1(dr91)*. To create mutant combinations, we used either standard genetic crossing approaches or CRISPR/Cas9 genetic engineering (see below for CRISPR methods). The homozygous genotype of every strain was confirmed either by DNA sequencing of the mutant lesion, restriction digest, or a loss of function phenotype.

## Genetic methods

ENU mutagenesis and mutant isolation: L4 stage *drls4* animals ( $P_0$ ) were mutagenized in 0.6 mM N-ethyl-N-nitrosourea (ENU) diluted in M9 for 4 hours at 20°C. One day after ENU mutagenesis, F<sub>1</sub> mutagenized eggs were isolated by hypochlorite solution and hatched on NGM plates overnight. Starved ENU mutagenized F<sub>1</sub> *drls4* L1 animals were washed twice in 1 x M9 and seeded onto 3 - 16 10 cm OP50 NGM plates. F<sub>2</sub> synchronized larvae were obtained via hypochlorite synchronization and seeded onto OP50 NGM plates. Day one adult F<sub>2</sub> *drls4* animals were transferred to 250 mM NaCl OP50 NGM plates for 18 hours. As controls, unmutagenized *drls4* day 1 adults were also transferred to 50 mM NaCl and 250 mM NaCl OP50 NGM plates for 18 hours. After 18 hours, RFP and GFP fluorescence intensity, time of flight (TOF), and extinction (EXT) were acquired for each animal using a COPAS Biosort (Union Biometrica, Holliston, MA). Using the unmutagenized 50 mM NaCl NGM data as a reference, gate and sort regions for animals exposed to 250 mM NaCl were defined that isolated rare mutant animals with GFP and RFP levels similar to the population of unmutagenized *drls4* animals on 50 mM NaCl. These mutants were termed *nio* mutants (no induction of osmolyte biosynthesis gene expression). Individual *nio* mutant hermaphrodites were selfed and their F<sub>3</sub> and F<sub>4</sub> progeny re-tested to confirm the Nio phenotype.

Backcrossing and single gene recessive determination: Each *nio* mutant was backcrossed to *drls4* males three times. F<sub>1</sub> progeny from these backcrosses were tested on 250 mM NaCl for 18 hours as day 1 adults. As expected for a recessive mutant, 100% of the crossed progeny were WT (non-*nio*). F<sub>1</sub> heterozygous hermaphrodites from these crosses were selfed and their progeny (F<sub>2</sub>) were tested on 250 mM NaCl for 18 hours as day 1

adults. As expected for a single gene recessive mutation, ~25% of progeny exhibited the Nio phenotype (Table S1).

Complementation testing: *nio/+* males were crossed with hermaphrodites homozygous for the mutation being complementation tested. The F<sub>1</sub> progeny from this cross were put on 250 mM NaCl OP50 NGM plates for 18 hours and screened for complementation. Crosses in which ~50% of these F<sub>1</sub> progeny were WT failed to complement (i.e. were alleles of the same gene). Crosses in which 100% of these F<sub>1</sub> progeny were WT complemented (i.e. represented alleles of different genes). Each mutant was complementation tested to every other mutant twice – as both a hermaphrodite and as a male.

Whole genome sequencing: DNA was isolated from starved OP50 NGM plates with WT(*drls4*) or mutant animals using the Qiagen Gentra Puregene Tissue Kit (Cat No 158667). The supplementary protocol for “Purification of archive-quality DNA from nematode suspensions using the Gentra Puregene Tissue Kit” available from Qiagen was used to isolate DNA. DNA samples were sequenced by BGI Americas (Cambridge, MA) with 20X coverage and paired-end reads using the Illumina HiSeq X Ten System.

SNP and INDEL Identification in Mutants: A Galaxy workflow was used to analyze the FASTQ forward and reverse reads obtained from BGI. The forward and reverse FASTQ reads from the animal of interest, *C. elegans* reference genome Fasta file (ce11m.fa), and SnpEff download gene annotation file (SnpEff4.3 WBcel235.86) were input into the Galaxy workflow. The forward and reverse FASTQ reads were mapped to the reference genome Fasta files with the Burrows-Wheeler Aligner (BWA) for Illumina. The resultant Sequence

Alignment Map (SAM) dataset was filtered using bitwise flag and converted to the Binary Alignment Map (BAM) format (47). Read groups were added or replaced in the BAM file to ensure proper sequence analysis by downstream tools. To identify areas where the sequenced genome varied from the reference genome, the Genome Analysis Toolkit (GATK) Unified Genotyper was used. The types of variants identified with GATK were Single Nucleotide Polymorphisms (SNPs) and Insertion and Deletions (INDELs). The SnpEff4.3 WBcel235.86 gene annotation file was used to annotate the non-synonymous SNPs and INDELs that were identified as variants by GATK. The final list of all variants with annotated non-synonymous variants was exported as a Microsoft Excel table. To identify mutations in the sequenced mutants that were not in the parent strain (*drls4*), the MATCH and VLOOKUP functions in Microsoft Excel were used.

### **COPAS Biosort Acquisition and Analysis**

Day one adults from a synchronized egg lay or hypochlorite preparation were seeded on 50 or 250 mM NaCl OP50 or the indicated RNAi NGM plates. After 18 hours, the GFP and RFP fluorescence intensity, time of flight (TOF), and extinction (EXT) of each animal was acquired with the COPAS Biosort. Events in which the RFP intensity of adult animals (TOF 400-1200) was <20 (dead worms or other objects) were excluded from the analysis. The GFP fluorescence intensity of each animal was normalized to its RFP fluorescence intensity or TOF. To determine the fold induction of GFP for each animal, each GFP/RFP or GFP/TOF was divided by the average GFP/RFP or GFP/TOF of that strain exposed to 50 mM NaCl. The relative fold induction was determined by setting the fold induction of *drls4* exposed to 250 mM NaCl to 1. Each graphed point represents the quantified signal from a single animal.

## Molecular Biology and Transgenics

Reporter strains: The *drls4* strain was made by injecting wild type animals with *gpdh-1p::GFP* (20ng/μL) and *col-12p::dsRed2* (100ng/μL) to generate the extrachromosomal array *drEx73*, which was integrated using UV bombardment, followed by isolation of animals exhibiting 100% RFP fluorescence. The resulting strain was outcrossed five times to wild type to generate the homozygous integrated transgene *drls4*. *kbls6* was generated from a Gene Gun bombardment of *unc-119(ed3)* animals with a *gpdh-1p::gpdh-1::GFP* plasmid and an *unc-119(+)* rescue plasmid (pMM051). The resulting strain was outcrossed five times to generate *kbls6*. *drls4* is integrated on LGIV. The integration site for *kbls6* is unmapped.

Transgene rescue: All the primers used to generate the rescue constructs can be found in Table S5. The genomic *ogt-1* rescue construct (used in the *drEx465* extrachromosomal array) was made by amplifying *ogt-1* with 2 kb of sequence upstream of the start codon and 1 kb of sequence downstream of the stop codon. All other rescue constructs (used in extrachromosomal arrays *drEx468* – *drEx474*) were made using Gibson Assembly. The *ogt-1* promoter, *ogt-1* cDNA, and *ogt-1* 3'utr were cloned into the *pPD61.125* vector through a four component Gibson Assembly reaction. This vector was used as the backbone for all other promoter and human OGT rescue constructs. All rescue constructs were confirmed by Sanger sequencing. Extrachromosomal array lines were made by injecting day one adult animals with the rescue construct (20 ng/μL) and *rol-6(su1006)* (100 ng/μL).

CRISPR/Cas9 genomic editing: CRISPR allele generation was preformed using the single-stranded oliodeoxynucleotide donors (ssODN) method (48). gRNA and repair

template sequences are found in Table S5. For identification of the *dr20* allele, we performed RFLP analysis using the *MboI* restriction enzyme, which cuts the WT allele, but not *dr20*. For identification of the *dr86*, *dr89*, *dr90*, and *dr91* alleles, we performed RFLP analysis using the *DdeI* restriction enzyme, which cuts the mutant alleles, but not WT. To make the *gpdh-1::GFP* CRISPR strain, we used a previously described double stranded DNA (dsDNA) asymmetric-hybrid donor method (48). To make the *ogt-1::GFP* CRISPR strain, we used a dsDNA donor method using Sp9 modified primers (49). Homozygous CRISPR/Cas9 generated alleles were isolated by selfing heterozygotes to ensure that complex alleles were not obtained.

mRNA isolation, cDNA synthesis, and qPCR: Day one animals were plated on 50 mM or 250 mM NaCl OP50 NGM plates for 24 hours. Unless noted otherwise, after 24 hours, 35 animals were picked into 50  $\mu$ L Trizol for mRNA isolation. RNA isolation followed a combined Trizol/RNeasy column purification method as previously described (11). cDNA was synthesized from total RNA using the SuperScript VILO Master Mix. SYBER Green master mix, 2.5 ng cDNA, and the primers listed in Table S5 were used for each qPCR reaction. qPCR reactions were carried out using an Applied Biosystems 7300 Real Time PCR machine. *act-2* primers were used as a control for all qPCR reactions. At least three biological replicates of each qPCR reaction were carried with three technical replicates per biological replicate. qPCR data was analyzed through  $\Delta\Delta C_t$  analysis with all samples normalized to *act-2*. Data are represented as fold induction of RNA on 250 mM NaCl relative to on 50 mM NaCl.

Western Blots: Cell lysates were prepared from hypochlorite synchronized day 1 adult animals exposed to 50 mM or 250 mM NaCl plates for 18 hours. 3-5 non-starved 10 cm

plates were concentrated into a 100  $\mu$ L mixture. NuPage LDS Sample Buffer (4X) and NuPAGE Sample Reducing Agent (10X) were added and the sample was frozen and thawed three times at -80°C and 37°C. Prior to get loading, the sample was heated to 100°C for 10 minutes and cleared by centrifugation at 4°C, 12,000 x g for 15 minutes. The cleared supernatant was run on a Blot 4-12% or 8% Bis-Tris Mini Plus gel and transferred to a nitrocellulose membrane using iBlot 2 NC Regular Stacks and the iBlot 2 Dry Blotting System. The membranes were placed on iBind cards and the iBind western device was used for the antibody incubation and blocking. The Flex Fluorescent Detection (FD) Solution Kit or the iBind Solution Kit was used to dilute the antibodies and block the membrane. The antibodies used are listed in Table S7. The following antibody dilutions were used: 1:1000  $\alpha$ -GFP, 1:2000  $\alpha$ - $\beta$ -Actin, 1:2000  $\alpha$ -mouse HRP, and 1:4000 Goat  $\alpha$ -Mouse IgG (H+L) Cross-Absorbed Secondary DyLight 800. A C-DiGit Licor Blot Scanner (LI-COR Biosciences, Lincoln, NE) or an Odyssey CLx imaging System (LI-COR Biosciences, Lincoln, NE) were used to image membranes incubated with a chemiluminescent or fluorescent secondary antibody, respectively.

## Microscopy

Worms were anesthetized (10mM levamisole) and mounted on agar plates for widefield fluorescence microscopy. Images were collected on a Leica MZ16FA stereo dissecting scope with a DFC345 FX camera (Leica Microsystems, Wetzlar, Germany). Unless noted, images within an experiment were collected using the same exposure and zoom settings. Unless noted, images depict merged GFP and RFP channels of age matched day 2 adult animals exposed to 50 or 250 mM NaCl for 18 hours.

## Immunofluorescence

Embryos from a hypochlorite preparation were freeze-cracked on a superfrost slide, fixed with paraformaldehyde, blocked with bovine serum albumin (BSA), incubated with a 1:400 dilution of  $\alpha$ -O-GlcNAc monoclonal antibody (RL2) overnight, and incubated with 1:400 dilution of 1:400 goat  $\alpha$ -mouse IgG, IgM (H+L) Secondary Antibody, Alexa Fluor 488 for 4 – 6 hours. The antibodies used are listed in Table S7. Washes with PBS or antibody buffer were carried out between each incubation step. Images were collected on a Leica MZ16FA stereo dissecting scope with a DFC345 FX camera (Leica Microsystems, Wetzlar, Germany). Images were taken with the same zoom settings, but different exposure settings.

### ***C. elegans* Assays**

Adaptation Assay: Day one adult animals were transferred to five 50 mM NaCl OP50 NGM plates and five 200 mM NaCl OP50 plates. ~25 animals were transferred to each plate. After 24 hours, 20 animals from each 50 mM or 200 mM plate were transferred to 600 mM NaCl OP50 NGM plates. Animals were scored for movement after 24 hours on the 600 mM NaCl OP50 NGM plates. To be counted as moving, the animal had to move greater than half a body length. Animals that were not moving were lightly tapped on the nose to confirm that they were paralyzed or dead. Survival assays and osmotic stress resistance (Osr) assays were performed as previously described (11).

### **Statistical Analysis**

Comparisons of means were analyzed with either a two-tailed Students t-test (2 groups) or ANOVA (3 or more groups) using the Dunnett's or Tukey's post-test analysis as indicated in GraphPad Prism 7 (GraphPad Software, Inc., La Jolla, CA). p-values of

<0.05 were considered significant. Data are expressed as mean  $\pm$  S.D. with individual points shown.

## Acknowledgements

This work was supported by grants from the NIH (R01GM105655 to T.L.)). Some strains were provided by the CGC, which is funded by NIH Office of Research Infrastructure Programs (P40 OD010440). We thank the lab of Gary Ruvkun (Harvard) for the Galaxy whole genome sequencing workflow, the lab of Oliver Hobert (Columbia) for providing additional *ogt-1* strains, and David Raizen (UPenn) for critical reading of the manuscript.

## **Author Contributions**

Conceptualization, T.L. and S.J.U.; Methodology, T.L. and S.J.U; Investigation, S.J.U. and M.C., Resources, J.A.H.; Writing - Original Draft, T.L. and S.J.U.; Writing – Review and Editing, T.L. and J.A.H.; Visualization, S.J.U.; Supervision, T.L.; Funding Acquisition, T.L.

## **Declaration of Interests**

The authors declare no competing interests.

## Figure legends

### Figure 1. *gpdh-1* transcriptional and translational reporters are upregulated by hypertonic stress.

- (A) Wide-field fluorescence microscopy of day 2 adult animals expressing *drls4* (*col-12p::dsRed*; *gpdh-1p::GFP*) exposed to 50 or 250 mM NaCl NGM plates for 18 hours. Images depict merged GFP and RFP channels. Scale bar = 100 microns.
- (B) COPAS Biosort quantification of GFP and RFP signal in day 2 adult animals expressing *drls4* exposed to 50 or 250 mM NaCl NGM plates for 18 hours. Each point represents the quantified signal from a single animal.  $N \geq 276$  for each group.
- (C) Population mean of the normalized GFP/RFP ratio from data in 1B. Data are expressed as mean  $\pm$  S.D. with individual points shown. \*\*\*\* -  $p < 0.0001$  (Student's T-test)
- (D) Wide-field fluorescence microscopy of day 2 adult animals expressing a *kbls6* (*gpdh-1p::GPDH-1-GFP*) translational fusion protein exposed to 50 or 250 mM NaCl NGM plates for 18 hours. Scale bar = 100 microns.
- (E) COPAS Biosort quantification of GFP and TOF signal in day 2 adult animals expressing the *kbls6* translational fusion protein exposed to 50 or 250 mM NaCl NGM plates for 18 hours.  $N \geq 276$  for each group.
- (F) Population mean of the normalized GFP/TOF ratio from data in 1E. Data are expressed as mean  $\pm$  S.D. \*\*\*\* -  $p < 0.0001$  (Student's T-test).

**Figure 2. The conserved O-GlcNAc transferase OGT-1 is required for the upregulation of the *gpdh-1* transcriptional reporter by hypertonic stress.**

(A) ENU-based forward genetic screening strategy and mutant identification workflow.

(B) *C. elegans* OGT-1 and *Homo sapiens* OGT protein domain diagrams detailing the positions of the two LOF *ogt-1* alleles identified in the screen (*dr15* and *dr20*), two independently isolated *ogt-1* deletion mutations (*ok430* and *ok1474*), and two mutations that disrupt catalytic activity of the enzyme (H612A and K957M). The precise breakpoints of *ok1474* have not been determined.

(C) Wide-field fluorescence microscopy of day 2 adult *drls4* and *ogt-1;drls4* mutant animals exposed to 50 or 250 mM NaCl NGM plates for 18 hours. Images depict merged GFP and RFP channels. Scale bar = 100 microns.

(D) COPAS Biosort quantification of GFP and RFP signal in day 2 adult animals expressing *drls4* or *ogt-1;drls4* exposed to 50 or 250 mM NaCl NGM plates for 18 hours. Data are represented as the relative fold induction of normalized GFP/RFP ratio on 250 mM NaCl NGM plates versus 50 mM NaCl NGM plates, with WT fold induction set to 1. Each point represents the quantified signal from a single animal. Data are expressed as mean  $\pm$  S.D. \*\*\*\* -  $p < 0.0001$  (One-way ANOVA with post hoc Dunnett's test).  $N \geq 62$  for each group.

(E) COPAS Biosort quantification of GFP and RFP signal in day 2 adult animals expressing *drls4* or *drls4;ogt-1(dr20)* exposed to 50 or 250 mM NaCl NGM plates for 18 hours. *ogt-1(dr20 dr36)* is a strain in which the *dr20* mutation is converted back to WT using CRISPR/Cas9 genome editing. Data are represented as relative fold induction of normalized GFP/RFP ratio on 250 mM NaCl NGM plates versus 50 mM NaCl NGM plates, with WT fold induction set to 1. Each point represents the quantified signal from a single animal. Data are expressed as mean  $\pm$  S.D. \*\*\*\* -  $p < 0.0001$  (One-way ANOVA

with post hoc Dunnett's test).  $N \geq 170$  for each group. *Inset*: Wide-field fluorescence microscopy of day 2 adult animals expressing *drls4* in the WT or indicated *ogt-1* mutant background exposed to 250 mM NaCl NGM plates for 18 hours. Images depict merged GFP and RFP channels. Scale bar = 100 microns.

(F) COPAS Biosort quantification of GFP and RFP signal in day 2 adult animals expressing *drls4* exposed to 50 or 250 mM NaCl NGM plates for 18 hours. Animals were placed on *empty vector(RNAi)* (*ev(RNAi)*) or *ogt-1(RNAi)* plates at the indicated stage. Data are represented as normalized fold induction of normalized GFP/RFP ratio on 250 mM NaCl RNAi plates relative to on 50 mM NaCl RNAi plates, with *ev(RNAi)* set to 1 for each RNAi timepoint. Each point represents the quantified signal from a single animal. Data are expressed as mean  $\pm$  S.D. \*\*\*\* -  $p < 0.0001$  (Student's two-tailed T-test)  $N \geq 144$  for each group.

### Figure 3. OGT-1 functions post-transcriptionally to regulate osmosensitive protein expression.

(A) qPCR of *gpdh-1*, *hmit-1.1*, and *nlp-29* mRNA from WT and *ogt-1(dr20)* day 2 adult animals expressing *drIs4* exposed to 50 or 250 mM NaCl NGM plates for 24 hours.

Data are represented as fold induction of RNA on 250 mM NaCl relative to on 50 mM NaCl. Data are expressed as mean  $\pm$  S.D. \*\* -  $p < 0.01$ , n.s. = nonsignificant (Student's two-tailed t-test).  $N \geq 3$  biological replicates of 35 animals for each group.

(B) qPCR of *GFP* mRNA from WT and *ogt-1(dr20)* day 2 animals expressing *drIs4* exposed to 50 or 250 mM NaCl NGM plates for 24 hours. Data are represented as fold induction of RNA on 250 mM NaCl relative to on 50 mM NaCl. Data are expressed as mean  $\pm$  S.D. \* -  $p < 0.05$  (Student's two-tailed t-test).  $N \geq 3$  biological replicates of 35 animals for each group.

(C) COPAS Biosort quantification of GFP and TOF signal in day 2 adult animals expressing the *kbIs6* GPDH-1 translational fusion exposed to 50 or 250 mM NaCl NGM plates for 18 hours. The *ogt-1(dr34)* allele carries the same homozygous Q600STOP mutation as the *ogt-1(dr20)* allele and was introduced using CRISPR/Cas9. Data are represented as relative fold induction of normalized GFP/TOF ratio on 250 mM NaCl NGM plates versus 50 mM NaCl NGM plates. Each point represents the quantified signal from a single animal. Data are expressed as mean  $\pm$  S.D. \*\*\*\* -  $p < 0.0001$  (Student's two-tailed t-test).  $N \geq 84$  for each group. *Inset*: Wide-field fluorescence microscopy of day 2 adult animals expressing the *kbIs6* translational fusion protein exposed to 250 mM NaCl NGM plates for 18 hours. Scale bar = 100 microns.

(D) qPCR of *gpdh-1* mRNA from day 2 adult animals expressing the *kbIs6* translational fusion exposed to 50 or 250 mM NaCl NGM plates for 24 hours. Strains include WT and *ogt-1(dr34)*. The *ogt-1(dr34)* allele is the *dr20* point mutation introduced using

CRISPR/Cas9. Data are represented as fold induction of RNA on 250 mM NaCl relative to on 50 mM NaCl. Data are expressed as mean  $\pm$  S.D. n.s. = nonsignificant (Student's two-tailed t-test). N = 3 biological replicates of 35 animals for each group.

(E) Immunoblot of GFP and  $\beta$ -actin in lysates from day 2 adult animals exposed to 50 mM or 250 mM NaCl for 18 hours. The animals express a CRISPR/Cas9 edited knock-in of GFP into the endogenous *gpdh-1* gene (*gpdh-1(dr81)*). *ogt-1* carries the *dr83* allele, which is the same homozygous Q600STOP mutation as the *ogt-1(dr20)* allele and was introduced using CRISPR/Cas9. *Top*: Normalized quantification of immunoblots. \* -  $p < 0.05$  (One-way ANOVA with post hoc Dunnett's test). *Bottom*: Representative immunoblot. N = 3 biological replicates.

**Figure 4. *ogt-1* is required for physiological and genetic adaptation to hypertonic stress.**

(A) Percent of moving unadapted and adapted day 3 adult animals exposed to 600 mM NaCl NGM plates for 24 hours. Strains expressing *drIs4* are on the left of the dashed orange line and those not expressing *drIs4* are on the right. Data are expressed as mean  $\pm$  S.D. \*\*\*\* -  $p < 0.0001$ , \*\* -  $p < 0.01$  (One-way ANOVA with post hoc Dunnett's test). N = 5 replicates of 20 animals for each strain.

(B) COPAS Biosort quantification of GFP and RFP signal in day 2 adult animals expressing *drIs4* exposed to 50 mM NaCl NGM plates. Data are represented as the fold induction of normalized GFP/RFP ratio on 50 mM NaCl NGM plates, with *osm-8(dr9)* set to 1. *osm-8(dr9)* was isolated in a previous genetic screen for new *osm-8* alleles but encodes the same mutation as the *n1518* reference allele. Each point represents the quantified signal from a single animal. Data are expressed as mean  $\pm$  S.D. \*\*\*\* -  $p < 0.0001$  (Student's two-tailed t-test). N  $\geq$  109 for each group. *Inset*: Wide-field fluorescence microscopy of day 2 adult animals expressing *drIs4* exposed to 50 mM NaCl NGM plates. Images depict merged GFP and RFP channels. Scale bar = 100 microns.

(C) Percent of moving (OSR, osmotic stress resistant) day 1 animals after exposure to 500 mM NaCl or 700 mM NaCl for 10 minutes. Data are represented as mean  $\pm$  S.D. \*\*\*\* -  $p < 0.0001$  (Student's two-tailed t-test). N = 5 replicates of 10 animals for each strain.

**Figure 5. Non-canonical activity of *ogt-1* in the hypodermis regulates *gpdh-1* induction by hypertonic stress through a functionally conserved mechanism.**

(A) Wide-field fluorescence microscopy of day 2 adult animals expressing *drIs4* exposed to 50 or 250 mM NaCl NGM plates for 18 hours. Strains express an *ogt-1* cDNA from the indicated tissue-specific promoter. Images depict the GFP channel only for clarity. The RFP signal was unaffected in these rescue strains (not shown). Scale bar = 100 microns.

(B) COPAS Biosort quantification of GFP and RFP signal in day 2 adult animals expressing *drIs4* exposed to 50 or 250 mM NaCl NGM plates for 18 hours. Data are represented as the fold induction of normalized GFP/RFP ratio on 50 and 250 mM NaCl NGM plates relative to on 50 mM NaCl NGM plates. Each point represents the quantified signal from a single animal. Data are expressed as mean  $\pm$  S.D. \*\*\*\* -  $p < 0.0001$  (One-way ANOVA with post hoc Dunnett's test).  $N \geq 37$  for each group.

(C) Wide-field fluorescence microscopy of day 2 adult animals expressing *drIs4* exposed to 50 or 250 mM NaCl NGM plates for 18 hours. For the WT and catalytically inactive human rescue strains, we expressed a human cDNA corresponding to isoform 1 of OGT using an extrachromosomal array. Images depict the GFP channel for clarity. The RFP signal was unaffected in these rescue strains (not shown). Scale bar = 100 microns.

(D) COPAS Biosort quantification of GFP and RFP signal in day 2 adult animals expressing *drIs4* exposed to 50 or 250 mM NaCl NGM plates for 18 hours. Data are represented as the fold induction of normalized GFP/RFP ratio on 50 and 250 mM NaCl NGM plates relative to on 50 mM NaCl NGM plates. Each point represents the quantified signal from a single animal. Data are expressed as mean  $\pm$  S.D. \*\*\*\* -  $p < 0.0001$ , \*\* -  $p < 0.01$  (One-way ANOVA with post hoc Tukey's test).  $N \geq 40$  for each group.

(E) Wide-field fluorescence microscopy of day 2 adult animals expressing *dr/s4* exposed to 50 or 250 mM NaCl NGM plates for 18 hours. Images depict the GFP channel only for clarity. The RFP signal was unaffected in these rescue strains (not shown). Scale bar = 100 microns.

(F) COPAS Biosort quantification of GFP and RFP signal in day 2 adult animals expressing *dr/s4* exposed to 50 or 250 mM NaCl NGM plates for 18 hours. Data are represented as the fold induction of normalized GFP/RFP ratio on 50 and 250 mM NaCl NGM plates relative to on 50 mM NaCl NGM plates. Each point represents the quantified signal from a single animal. Data are expressed as mean  $\pm$  S.D. \*\*\*\* -  $p < 0.0001$  (One-way ANOVA with post hoc Dunnett's test).  $N \geq 81$  for each group.

(G) Percent of moving unadapted and adapted day 3 adult animals expressing *dr/s4* exposed to 600 mM NaCl NGM plates for 24 hours. Data are expressed as mean  $\pm$  S.D. \*\*\*\* -  $p < 0.0001$ , \*\* -  $p < 0.01$  (One-way ANOVA with post hoc Tukey's test).  $N = 5$  replicates of 20 animals for each strain.

**Figure 6. A non-catalytic function of *ogt-1* is required to couple hypertonic stress induced transcription and translation to enable physiological adaptation to hypertonic stress.**

(A) In WT, animals exposed to hypertonic stress induce the transcription of osmosensitive mRNAs, such as *gpdh-1*. These mRNAs are rapidly translated into protein by the ribosome, facilitating adaptation to hyperosmotic stress. Loss of *ogt-1* does not interfere with hypertonic stress induced transcription. Rather, loss of *ogt-1* decreases hypertonic stress induced protein levels. *ogt-1* may facilitate stress-induced translation via several potential mechanisms, including regulation of mRNA cleavage and 3'UTR usage, mRNA export, initiation factor interactions, or ribosomal elongation of the transcript. Importantly, the catalytic O-GlcNAcylation function of OGT-1 is not required in the hypertonic stress response.

## Supplemental Information

### Figure S1. *ogt-1* is required for upregulation of the transcriptional *gpdh-1::GFP* reporter (*drls4*) by hypertonic stress.

- (A) Immunoblot of GFP and  $\beta$ -actin in lysates from WT and *ogt-1* mutant animals expressing *drls4* exposed to 50 or 250 mM NaCl NGM plates for 18 hours.
- (B) COPAS Biosort quantification of GFP and RFP signal in day 2 adult WT animals expressing *drls4* exposed to 50 or 250 mM NaCl NGM plates for 18 hours. Animals were grown on *ev(RNAi)* or *ogt-1(RNAi)* plates for multiple generations. Data are represented as fold induction of normalized GFP/RFP ratio on 250 mM NaCl RNAi plates relative to on 50 mM NaCl RNAi plates. Each point represents the quantified signal from a single animal. Data are expressed as mean  $\pm$  S.D. \*\*\*\* -  $p < 0.0001$  (Student's T-test).  $N \geq 334$  for each group. *Inset*: Wide-field fluorescence microscopy of day 2 adult animals expressing *drls4* exposed to 250 mM NaCl NGM plates for 18 hours. Animals were grown on *ev(RNAi)* or *ogt-1(RNAi)* plates for multiple generations. Images depict merged GFP and RFP channels. Scale bar = 100 microns.
- (C) COPAS Biosort quantification of GFP and RFP signal in day 2 adult animals expressing *drls4* exposed to 50 or 250 mM NaCl NGM plates for 18 hours in the indicated genetic background. *drEx465* is an extrachromosomal array expressing a 10.3 Kb *ogt-1* genomic DNA fragment containing ~2Kb upstream and ~1Kb downstream of the *ogt-1* coding sequence. Data are represented as fold induction of normalized GFP/RFP ratio on 250 mM NaCl NGM plates relative to on 50 mM NaCl NGM plates. Each point represents the quantified signal from a single animal. Data are expressed as mean  $\pm$  S.D. \*\*\*\* -  $p < 0.0001$  (One-way ANOVA with post hoc Dunnett's test).  $N \geq 37$  for each group.

**Figure S2. *ogt-1* is not required for upregulation of transcriptional reporters by heat shock or ER stress.**

(A) Wide-field fluorescence microscopy of day 2 adult animals expressing *hsp-16.2p::GFP (gpls1)* grown on *ev(RNAi)*, *ogt-1(RNAi)*, or *hsf-1(RNAi)* plates and exposed to control or heat shock conditions (35°C for 3 hours, 18 hour recovery at 20°C). Images depict the GFP channel, since there is not a normalizing RFP reporter in these strains. Scale bar = 100 microns.

(B) COPAS Biosort quantification of GFP and TOF signal from animals in (A). Data are represented as fold induction of normalized GFP/TOF ratio of animals exposed to heat shock conditions relative to animals exposed to control conditions. Each point represents the quantified signal from a single animal. Data are expressed as mean  $\pm$  S.D. \*\*\*\* -  $p < 0.0001$  (One-way ANOVA with post hoc Dunnett's test).  $N \geq 158$  for each group.

(C) Wide-field fluorescence microscopy of day 2 adult animals expressing *hsp-4p::GFP (zcls4)* exposed to DTT plates for 18 hours. The *ogt-1(dr50)* allele carries the same homozygous Q600STOP mutation as the *ogt-1(dr20)* allele and was introduced using CRISPR/Cas9. Images depict the GFP channel. Scale bar = 100 microns.

(D) COPAS Biosort quantification of GFP and TOF signal from animals in (C). Data are represented as fold induction of normalized GFP/TOF ratio of animals exposed to DTT plates relative to animals exposed to control plates. Each point represents the quantified signal from a single animal. Data are expressed as mean  $\pm$  S.D. \*\*\*\* -  $p < 0.0001$  (One-way ANOVA with post hoc Dunnett's test).  $N \geq 48$  for each group.

**Figure S3. *ogt-1* is not required for upregulation of *gpdh-1* mRNA by hypertonic stress but is required for upregulation of GPDH-1 protein.**

(A) qPCR of *gpdh-1* mRNA in day 2 adult animals expressing *drIs4* exposed to 50 or 250 mM NaCl NGM plates for 3 hours. Strains include WT and *ogt-1(dr20)*. Data are represented as fold induction of RNA on 250 mM NaCl relative to on 50 mM NaCl. Data are expressed as mean  $\pm$  S.D. \*\* -  $p < 0.001$  (Student's two-tailed t-test). N = 3 biological replicates of 35 animals for each group.

(B) Immunoblot of GFP and  $\beta$ -actin in lysates from WT and *ogt-1(dr34)* animals expressing the *kbls6* translational fusion exposed to 50 or 250 mM NaCl NGM plates for 18 hours. The *ogt-1(dr34)* allele carries the same homozygous Q600STOP mutation as the *ogt-1(dr20)* allele and was introduced using CRISPR/Cas9. Numbers under the GFP bands represent GFP signal normalized to  $\beta$ -actin signal for each sample, with the WT 250 mM NaCl sample set to 1.

**Figure S4. *ogt-1* is not required for acute hypertonic stress survival but is required for chronic physiological and genetic adaptation to hypertonic stress.**

(A) Percent survival of day 2 adult animals expressing *drIs4* exposed to 100 - 600 mM NaCl NGM plates for 24 hours. Strains include WT, *ogt-1(dr15)*, and *ogt-1(dr20)*. Data are expressed as mean  $\pm$  S.D. N = 5 replicates of 20 animals for each salt concentration.

(B) Brightfield microscopy images of animals grown on 50 mM or 250 mM NaCl for 5 and 10 days respectively. Strains include WT (*drIs4*) and *ogt-1(dr20);drIs4*. Scale bar = 100 microns

(C) Percent of moving unadapted and adapted day 3 adult animals after exposure to 600 mM NaCl NGM plates for 24 hours. *ogt-1(dr20 dr36)* is a strain in which the *dr20* mutation was converted back to WT using CRISPR/Cas9 genome editing. The *gpdh-1(dr81)* allele is a CRISPR/Cas9 edited C-terminal knock-in of GFP into the endogenous *gpdh-1*. The *ogt-1(dr84)* allele is a CRISPR/Cas9 edited C-terminal knock-in of GFP into the endogenous *ogt-1*. Data are expressed as mean  $\pm$  S.D. \*\*\*\* -  $p < 0.0001$ , \*\* -  $p < 0.01$  (One-way ANOVA with post hoc Dunnett's test). N = 5 replicates of 20 animals for each strain.

(D) COPAS Biosort quantification of GFP and RFP signal in day 2 adult *drIs4* animals *drIs4* exposed to 50 mM NaCl NGM plates. Data are represented as the fold induction of normalized GFP/RFP ratio on 50 mM NaCl NGM plates, with *osm-11(n1604)* set to 1. The *ogt-1(dr52)* allele carries the same homozygous Q600STOP mutation as the *ogt-1(dr20)* allele, which was introduced using CRISPR/Cas9. Each point represents the quantified signal from a single animal. Data are expressed as mean  $\pm$  S.D. \*\*\*\* -  $p < 0.0001$  (Student's two-tailed t-test). N  $\geq$  163 for each group. *Inset*: Wide-field fluorescence microscopy of day 2 adult animals expressing *drIs4* exposed to 50 mM

NaCl NGM plates. Images depict merged GFP and RFP channels. Scale bar = 100 microns.

**Figure S5. OGT-1<sup>H612A</sup> and OGT-1<sup>K967M</sup> are expressed at wild type levels, exhibit normal subcellular localization and exhibit decreased or ablated levels of O-GlcNAcylation.**

(A) Wide-field fluorescence microscopy of day 1 adult animals expressing endogenously CRISPR/Cas9 GFP tagged OGT-1 exposed to 50 mM NaCl NGM plates. Scale bar = 100 microns. Images are exposure matched. *Inset*: Zoomed in images of the boxed area. Scale bar = 10 microns.

(B). Wide-field fluorescence microscopy of fixed and stained embryos. RL2 was used to stain for nuclear pore O-GlcNAc modifications and Hoechst 33258 was used to visualize the DNA. Images are not exposure matched in order to highlight the weak RL2 staining in OGT-1<sup>H612A</sup>. White arrowheads indicate RL2 staining in OGT-1 H612A embryos. Scale bar = 10 microns.

**Figure S6. Inhibition of proteasomal or autophagic pathways does not rescue *gpdh-1p::GFP* expression during hypertonic stress in *ogt-1(dr20)* mutants.**

(A) COPAS Biosort quantification of GFP and RFP signal in day 2 adult animals expressing *drls4* exposed to 50 or 250 mM NaCl NGM plates for 18 hours. Animals were placed on *empty vector(RNAi)* (*ev(RNAi)*) or *rpn-8(RNAi)* plates as L1s. Data are represented as normalized fold induction of normalized GFP/RFP ratio on 250 mM NaCl RNAi plates relative to on 50 mM NaCl RNAi plates. Each point represents the quantified signal from a single animal. Data are expressed as mean  $\pm$  S.D. \*\*\*\* -  $p < 0.0001$  (One-way ANOVA with post hoc Dunnett's test).  $N \geq 14$  for each group.

(B) COPAS Biosort quantification of GFP and RFP signal in day 2 adult animals expressing *drls4* exposed to 50 or 250 mM NaCl NGM plates for 18 hours. Animals were placed on *empty vector(RNAi)* (*ev(RNAi)*) or *lgg-1(RNAi)* plates as L1s. Data are represented as normalized fold induction of normalized GFP/RFP ratio on 250 mM NaCl RNAi plates relative to on 50 mM NaCl RNAi plates. Each point represents the quantified signal from a single animal. Data are expressed as mean  $\pm$  S.D. \*\*\*\* -  $p < 0.0001$  (One-way ANOVA with post hoc Dunnett's test).  $N \geq 47$  for each group.

**Table S1. *ogt-1(dr15)* and *ogt-1(dr20)* genetics are consistent with recessive and single gene alleles.**

\* Data not collected

**Table S2. All *ogt-1* alleles fail to complement for the Nio phenotype.**

**Table S3. Backcrossing does not substantially reduce the number of SNPs and INDELS in the *ogt-1(dr20)* strain.**

**Table S4. Strain used in this study**

**Table S5. DNA oligos used in this study**

**Table S6. Bacterial strains used in this study**

**Table S7. Chemicals, antibodies, peptides, and recombinant proteins**

**Table S8. Critical commercial assays**

## References

1. Burg MB. Molecular basis of osmotic regulation. *The American journal of physiology*. 1995;268(6 Pt 2):F983-96.
2. Terada Y, Inoshita S, Hanada S, Shimamura H, Kuwahara M, Ogawa W, et al. Hyperosmolality activates Akt and regulates apoptosis in renal tubular cells. *Kidney Int*. 2001;60(2):553-67.
3. Stookey JD, Pieper CF, Cohen HJ. Hypertonic hyperglycemia progresses to diabetes faster than normotonic hyperglycemia. *Eur J Epidemiol*. 2004;19(10):935-44.
4. Go WY, Liu X, Roti MA, Liu F, Ho SN. NFAT5/TonEBP mutant mice define osmotic stress as a critical feature of the lymphoid microenvironment. *Proceedings of the National Academy of Sciences of the United States of America*. 2004;101(29):10673-8.
5. Yancey PH. Compatible and counteracting solutes: protecting cells from the Dead Sea to the deep sea. *Sci Prog*. 2004;87(Pt 1):1-24.
6. Moronetti Mazzeo LE, Dersh D, Boccitto M, Kalb RG, Lamitina T. Stress and aging induce distinct polyQ protein aggregation states. *Proceedings of the National Academy of Sciences of the United States of America*. 2012;109(26):10587-92.
7. Lee SD, Choi SY, Lim SW, Lamitina ST, Ho SN, Go WY, et al. TonEBP stimulates multiple cellular pathways for adaptation to hypertonic stress: organic osmolyte-dependent and -independent pathways. *American journal of physiology Renal physiology*. 2011;300(3):F707-15.
8. Bagnasco SM, Uchida S, Balaban RS, Kador PF, Burg MB. Induction of aldose reductase and sorbitol in renal inner medullary cells by elevated extracellular NaCl. *Proc Natl Acad Sci U S A*. 1987;84(6):1718-20.
9. Lamitina ST, Morrison R, Moeckel GW, Strange K. Adaptation of the nematode *Caenorhabditis elegans* to extreme osmotic stress. *Am J Physiol Cell Physiol*. 2004;286(4):C785-91.
10. Lamitina T, Huang CG, Strange K. Genome-wide RNAi screening identifies protein damage as a regulator of osmoprotective gene expression. *Proc Natl Acad Sci U S A*. 2006;103(32):12173-8.
11. Rohlfing AK, Miteva Y, Hannenhalli S, Lamitina T. Genetic and physiological activation of osmosensitive gene expression mimics transcriptional signatures of pathogen infection in *C. elegans*. *PLoS One*. 2010;5(2):e9010.
12. Rohlfing AK, Miteva Y, Moronetti L, He L, Lamitina T. The *Caenorhabditis elegans* mucin-like protein OSM-8 negatively regulates osmosensitive physiology via the transmembrane protein PTR-23. *PLoS Genet*. 2011;7(1):e1001267.
13. Hart GW. Nutrient Regulation of Signaling & Transcription. *The Journal of biological chemistry*. 2019.
14. Olivier-Van Stichelen S, Hanover JA. You are what you eat: O-linked N-acetylglucosamine in disease, development and epigenetics. *Curr Opin Clin Nutr Metab Care*. 2015;18(4):339-45.
15. Capotosti F, Guernier S, Lammers F, Waridel P, Cai Y, Jin J, et al. O-GlcNAc transferase catalyzes site-specific proteolysis of HCF-1. *Cell*. 2011;144(3):376-88.

16. Daou S, Mashtalir N, Hammond-Martel I, Pak H, Yu H, Sui G, et al. Crosstalk between O-GlcNAcylation and proteolytic cleavage regulates the host cell factor-1 maturation pathway. *Proc Natl Acad Sci U S A*. 2011;108(7):2747-52.
17. Liu H, Gu Y, Qi J, Han C, Zhang X, Bi C, et al. Inhibition of E-cadherin/catenin complex formation by O-linked N-acetylglucosamine transferase is partially independent of its catalytic activity. *Mol Med Rep*. 2016;13(2):1851-60.
18. Giles AC, Desbois M, Opperman KJ, Tavora R, Maroni MJ, Grill B. A complex containing the O-GlcNAc transferase OGT-1 and the ubiquitin ligase EEL-1 regulates GABA neuron function. *J Biol Chem*. 2019;294(17):6843-56.
19. Kreppel LK, Blomberg MA, Hart GW. Dynamic glycosylation of nuclear and cytosolic proteins. Cloning and characterization of a unique O-GlcNAc transferase with multiple tetratricopeptide repeats. *J Biol Chem*. 1997;272(14):9308-15.
20. Lubas WA, Frank DW, Krause M, Hanover JA. O-Linked GlcNAc transferase is a conserved nucleocytoplasmic protein containing tetratricopeptide repeats. *J Biol Chem*. 1997;272(14):9316-24.
21. Pujol N, Cypowyj S, Ziegler K, Millet A, Astrain A, Goncharov A, et al. Distinct innate immune responses to infection and wounding in the *C. elegans* epidermis. *Curr Biol*. 2008;18(7):481-9.
22. Rahe DP, Hobert O. Restriction of Cellular Plasticity of Differentiated Cells Mediated by Chromatin Modifiers, Transcription Factors and Protein Kinases. *G3 (Bethesda)*. 2019;9(7):2287-302.
23. Lazarus MB, Nam Y, Jiang J, Sliz P, Walker S. Structure of human O-GlcNAc transferase and its complex with a peptide substrate. *Nature*. 2011;469(7331):564-7.
24. Lazarus MB, Jiang J, Kapuria V, Bhuiyan T, Janetzko J, Zandberg WF, et al. HCF-1 is cleaved in the active site of O-GlcNAc transferase. *Science*. 2013;342(6163):1235-9.
25. Hanover JA, Forsythe ME, Hennessey PT, Brodigan TM, Love DC, Ashwell G, et al. A *Caenorhabditis elegans* model of insulin resistance: altered macronutrient storage and dauer formation in an OGT-1 knockout. *Proc Natl Acad Sci U S A*. 2005;102(32):11266-71.
26. Shafi R, Iyer SP, Ellies LG, O'Donnell N, Marek KW, Chui D, et al. The O-GlcNAc transferase gene resides on the X chromosome and is essential for embryonic stem cell viability and mouse ontogeny. *Proc Natl Acad Sci U S A*. 2000;97(11):5735-9.
27. Love DC, Ghosh S, Mondoux MA, Fukushima T, Wang P, Wilson MA, et al. Dynamic O-GlcNAc cycling at promoters of *Caenorhabditis elegans* genes regulating longevity, stress, and immunity. *Proc Natl Acad Sci U S A*. 2010;107(16):7413-8.
28. Rahman MM, Stuchlick O, El-Karim EG, Stuart R, Kipreos ET, Wells L. Intracellular protein glycosylation modulates insulin mediated lifespan in *C.elegans*. *Aging (Albany NY)*. 2010;2(10):678-90.
29. Bond MR, Ghosh SK, Wang P, Hanover JA. Conserved nutrient sensor O-GlcNAc transferase is integral to *C. elegans* pathogen-specific immunity. *PLoS One*. 2014;9(12):e113231.

30. Ardiel EL, McDiarmid TA, Timbers TA, Lee KCY, Safaei J, Pelech SL, et al. Insights into the roles of CMK-1 and OGT-1 in interstimulus interval-dependent habituation in *Caenorhabditis elegans*. *Proc Biol Sci*. 2018;285(1891).
31. Taub DG, Awal MR, Gabel CV. O-GlcNAc Signaling Orchestrates the Regenerative Response to Neuronal Injury in *Caenorhabditis elegans*. *Cell Rep*. 2018;24(8):1931-8.e3.
32. Li H, Liu X, Wang D, Su L, Zhao T, Li Z, et al. O-GlcNAcylation of SKN-1 modulates the lifespan and oxidative stress resistance in *Caenorhabditis elegans*. *Sci Rep*. 2017;7:43601.
33. Mondoux MA, Love DC, Ghosh SK, Fukushima T, Bond M, Weerasinghe GR, et al. O-linked-N-acetylglucosamine cycling and insulin signaling are required for the glucose stress response in *Caenorhabditis elegans*. *Genetics*. 2011;188(2):369-82.
34. Kim Y, Choi J. Early life exposure of a biocide, CMIT/MIT causes metabolic toxicity via the O-GlcNAc transferase pathway in the nematode *C. elegans*. *Toxicol Appl Pharmacol*. 2019;376:1-8.
35. Hajduskova M, Baytek G, Kolundzic E, Gosdschan A, Kazmierczak M, Ofenbauer A, et al. MRG-1/MRG15 Is a Barrier for Germ Cell to Neuron Reprogramming in *Caenorhabditis elegans*. *Genetics*. 2019;211(1):121-39.
36. Guo B, Liang Q, Li L, Hu Z, Wu F, Zhang P, et al. O-GlcNAc-modification of SNAP-29 regulates autophagosome maturation. *Nat Cell Biol*. 2014;16(12):1215-26.
37. Shih PY, Lee JS, Shinya R, Kanzaki N, Pires-daSilva A, Badroos JM, et al. Newly Identified Nematodes from Mono Lake Exhibit Extreme Arsenic Resistance. *Curr Biol*. 2019;29(19):3339-44.e4.
38. Rouzaire-Dubois B, O'Regan S, Dubois JM. Cell size-dependent and independent proliferation of rodent neuroblastoma x glioma cells. *J Cell Physiol*. 2005;203(1):243-50.
39. Michea L, Ferguson DR, Peters EM, Andrews PM, Kirby MR, Burg MB. Cell cycle delay and apoptosis are induced by high salt and urea in renal medullary cells. *Am J Physiol Renal Physiol*. 2000;278(2):F209-18.
40. Pendergrass WR, Angello JC, Kirschner MD, Norwood TH. The relationship between the rate of entry into S phase, concentration of DNA polymerase alpha, and cell volume in human diploid fibroblast-like monokaryon cells. *Exp Cell Res*. 1991;192(2):418-25.
41. Gloster TM, Zandberg WF, Heinonen JE, Shen DL, Deng L, Vocadlo DJ. Hijacking a biosynthetic pathway yields a glycosyltransferase inhibitor within cells. *Nat Chem Biol*. 2011;7(3):174-81.
42. Pravata VM, Muha V, Gundogdu M, Ferenbach AT, Kakade PS, Vandadi V, et al. Catalytic deficiency of O-GlcNAc transferase leads to X-linked intellectual disability. *Proc Natl Acad Sci U S A*. 2019;116(30):14961-70.
43. Zhang X, Shu XE, Qian SB. O-GlcNAc modification of eIF4GI acts as a translational switch in heat shock response. *Nat Chem Biol*. 2018;14(10):909-16.
44. Jang I, Kim HB, Seo H, Kim JY, Choi H, Yoo JS, et al. O-GlcNAcylation of eIF2alpha regulates the phospho-eIF2alpha-mediated ER stress response. *Biochim Biophys Acta*. 2015;1853(8):1860-9.

45. Levine ZG, Walker S. The Biochemistry of O-GlcNAc Transferase: Which Functions Make It Essential in Mammalian Cells? *Annu Rev Biochem.* 2016;85:631-57.
46. Liu Y, Hengartner MO, Herr W. Selected elements of herpes simplex virus accessory factor HCF are highly conserved in *Caenorhabditis elegans*. *Mol Cell Biol.* 1999;19(1):909-15.
47. Li H, Handsaker B, Wysoker A, Fennell T, Ruan J, Homer N, et al. The Sequence Alignment/Map format and SAMtools. *Bioinformatics.* 2009;25(16):2078-9.
48. Dokshin GA, Ghanta KS, Piscopo KM, Mello CC. Robust Genome Editing with Short Single-Stranded and Long, Partially Single-Stranded DNA Donors in *Caenorhabditis elegans*. *Genetics.* 2018;210(3):781-7.
49. Ghanta KS, Dokshin GA, Mir A, Krishnamurthy PM, Gneid H, Edraki A, et al. 5' Modifications Improve Potency and Efficacy of DNA Donors for Precision Genome Editing. *bioRxiv.* 2018:354480.

# Figure 1

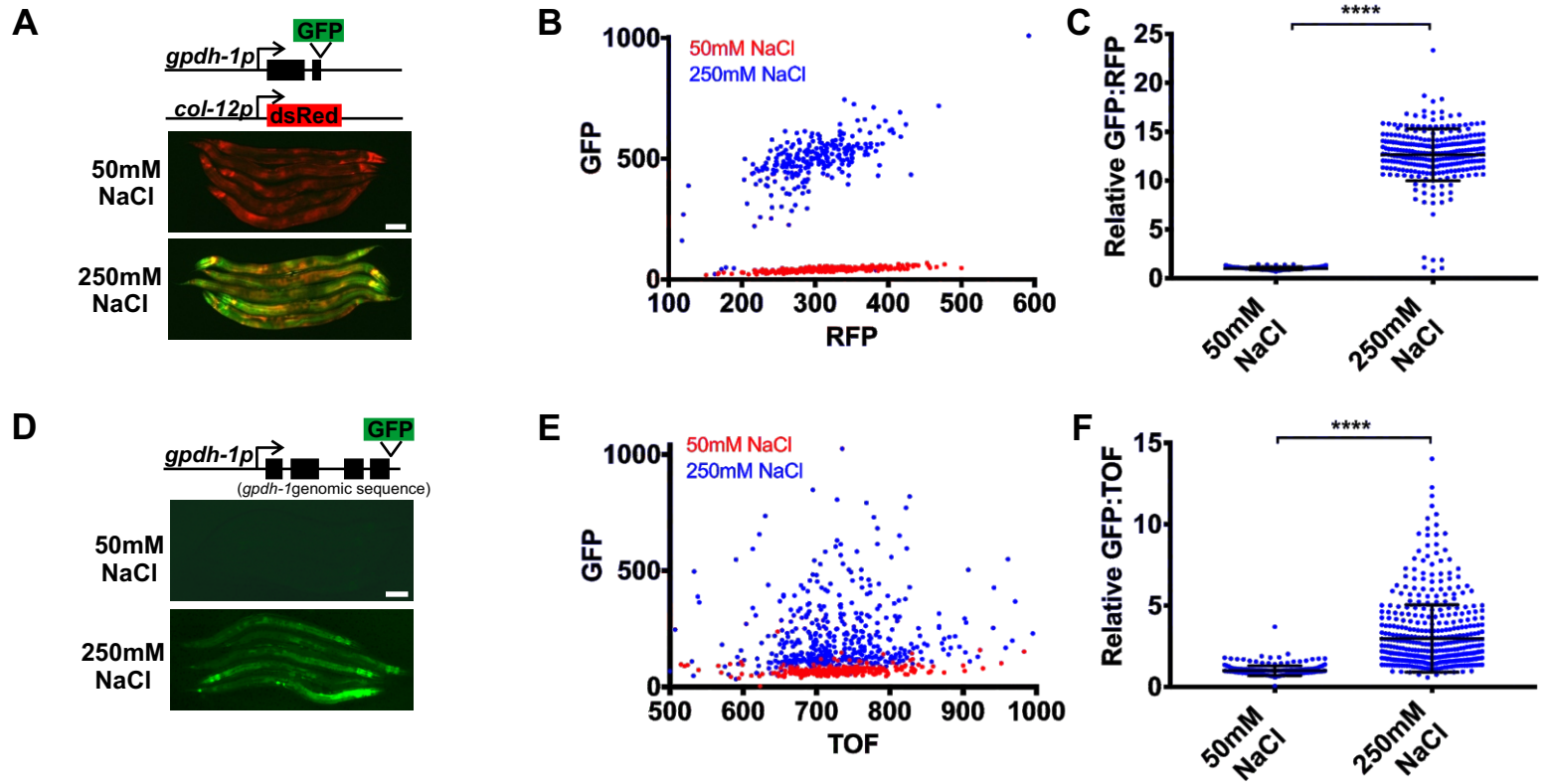


## Figure 2

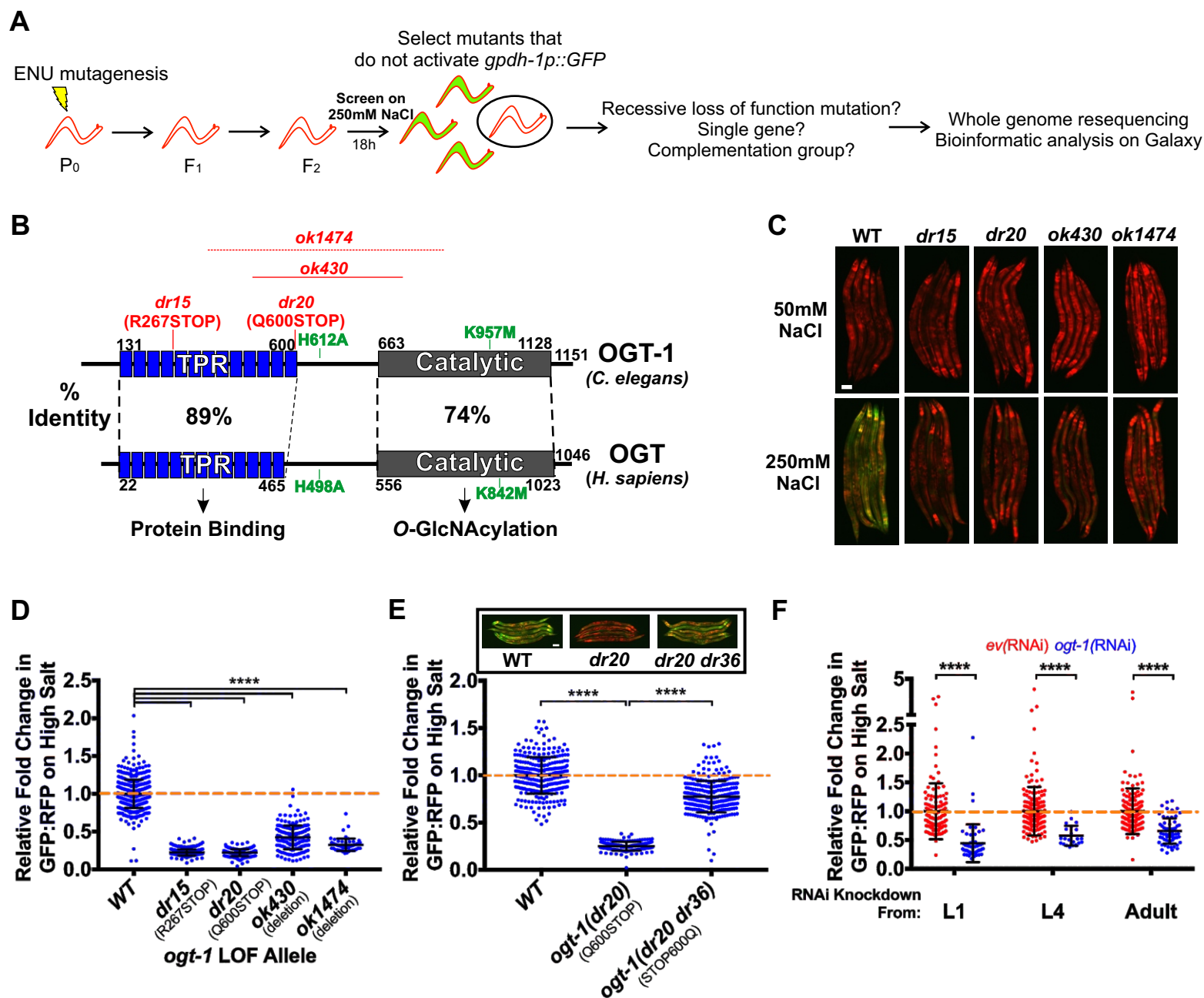


## Figure 3

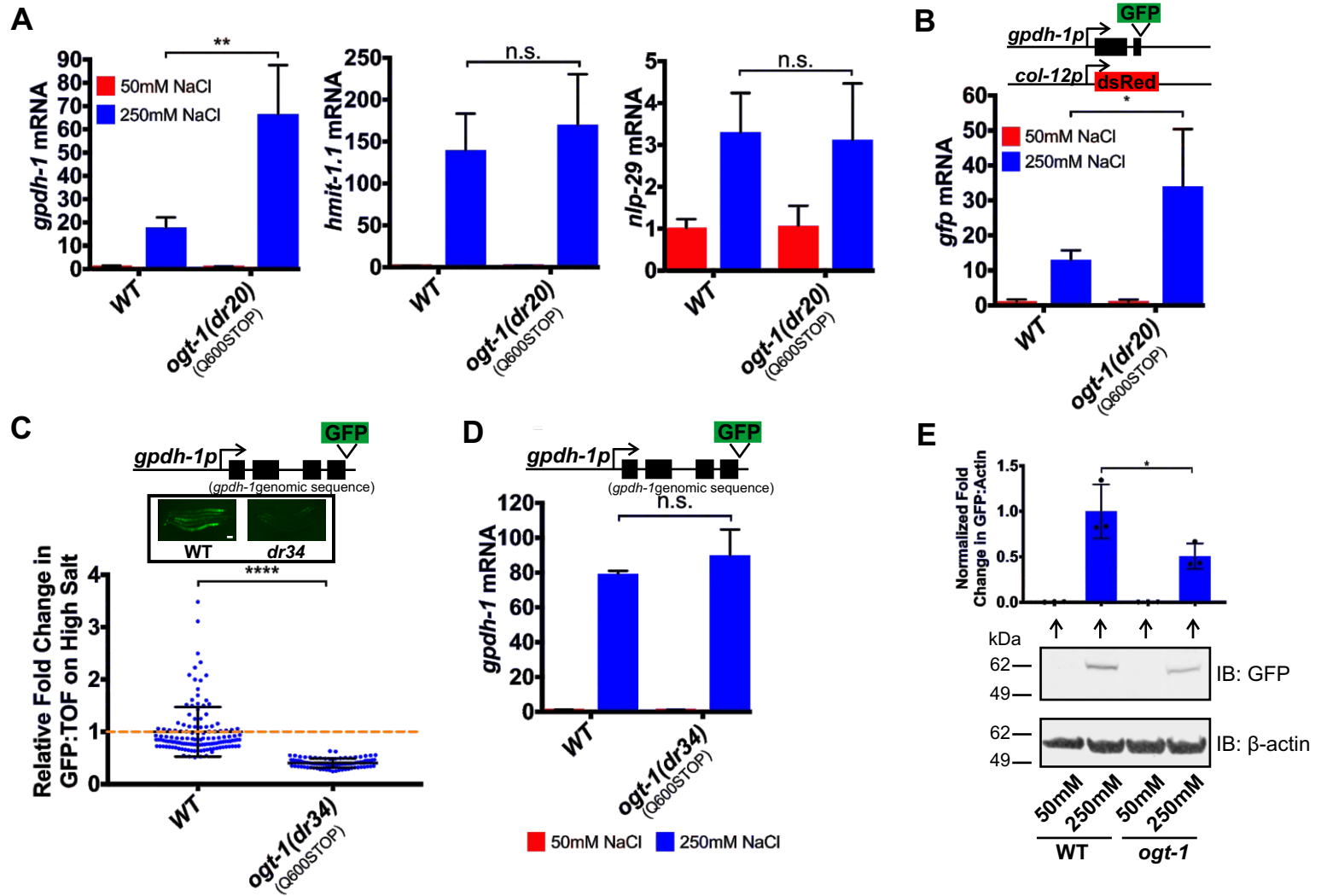


## Figure 4

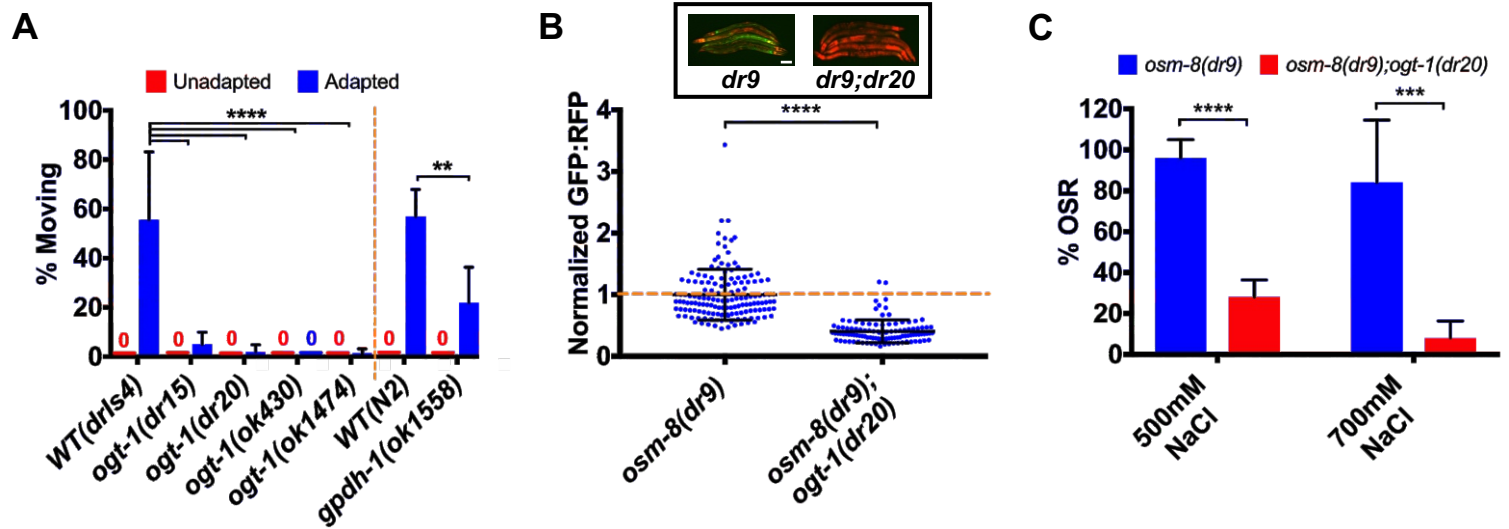


## Figure 5

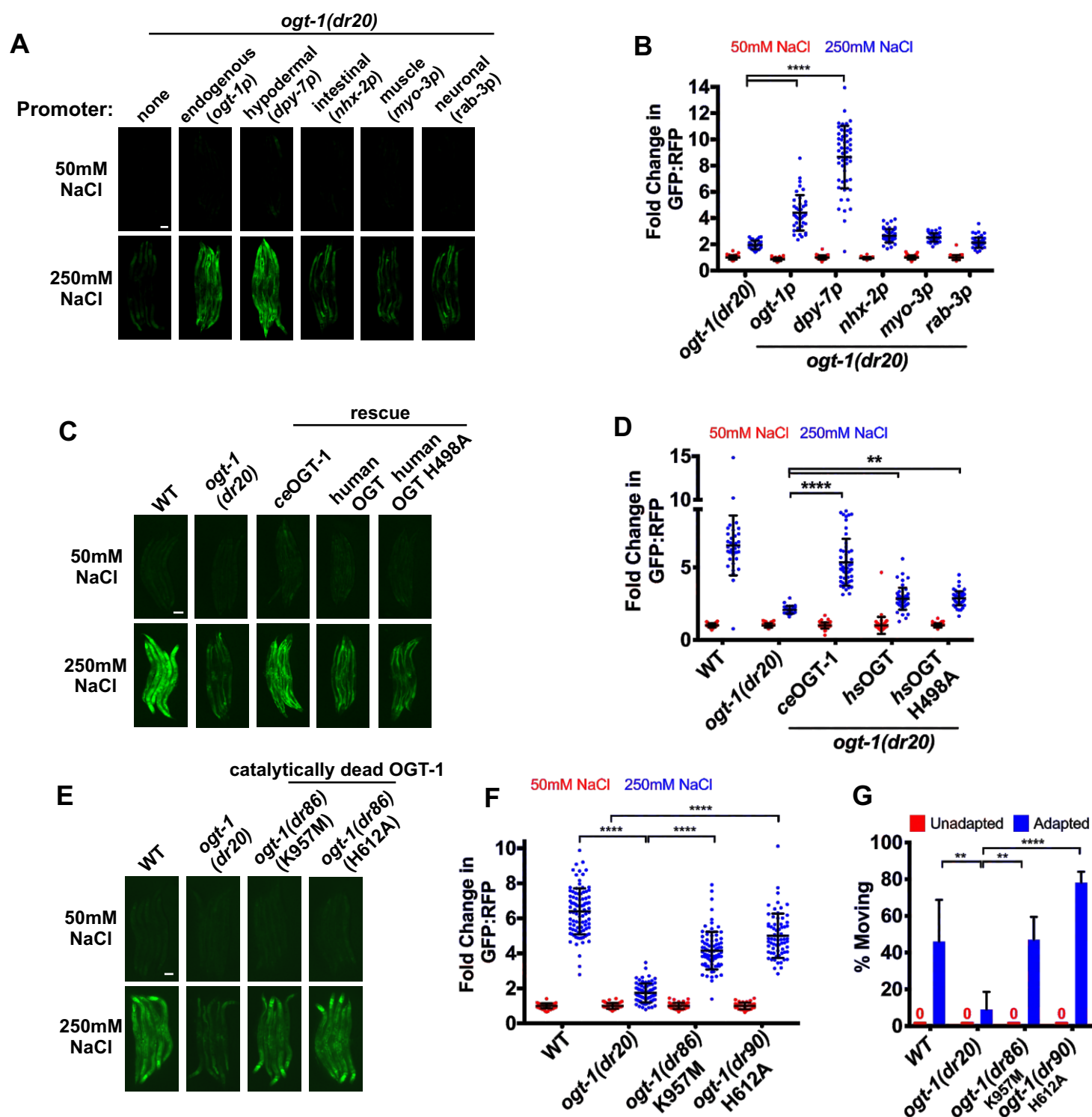


**Figure 6**

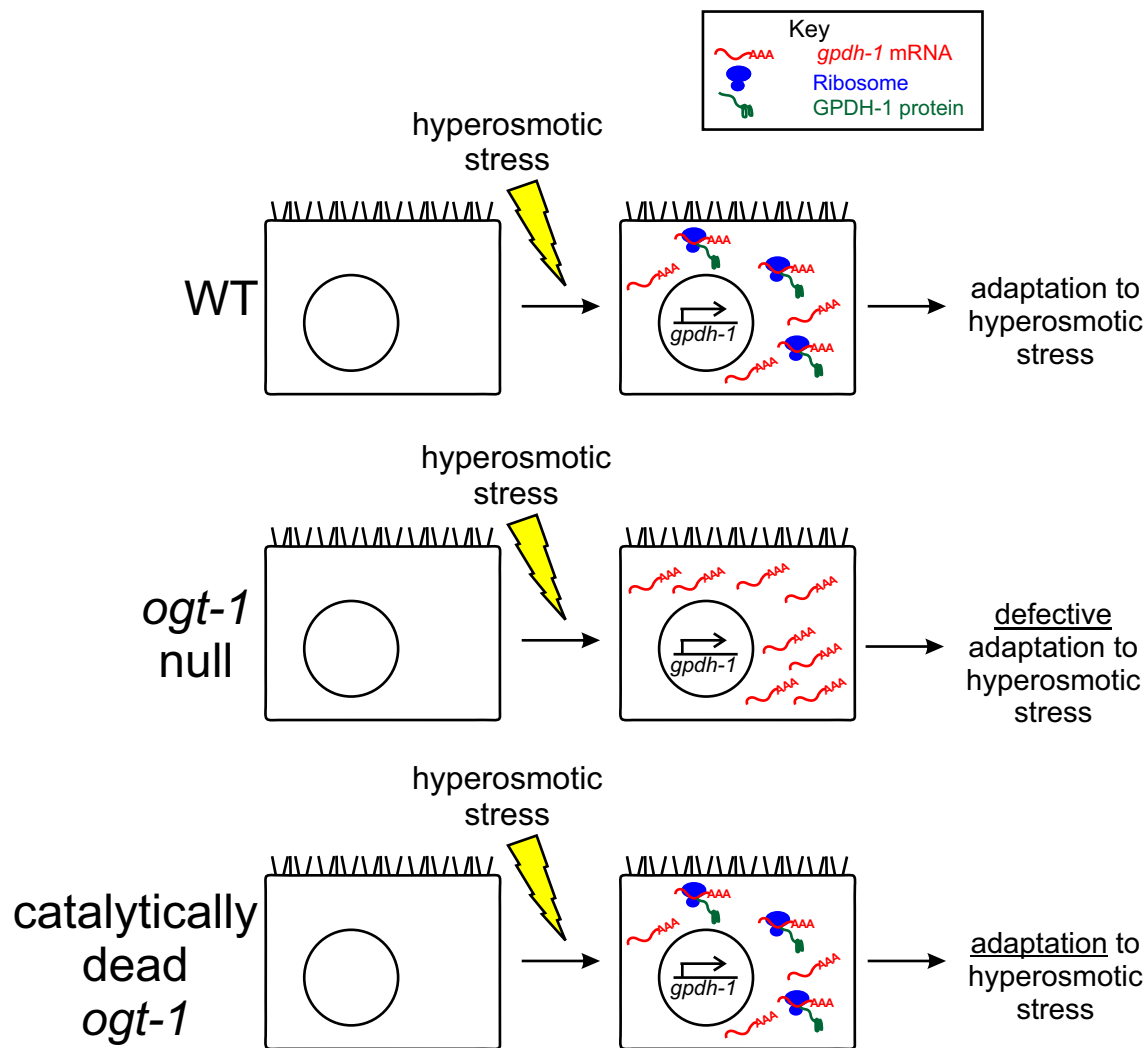


## Figure S1

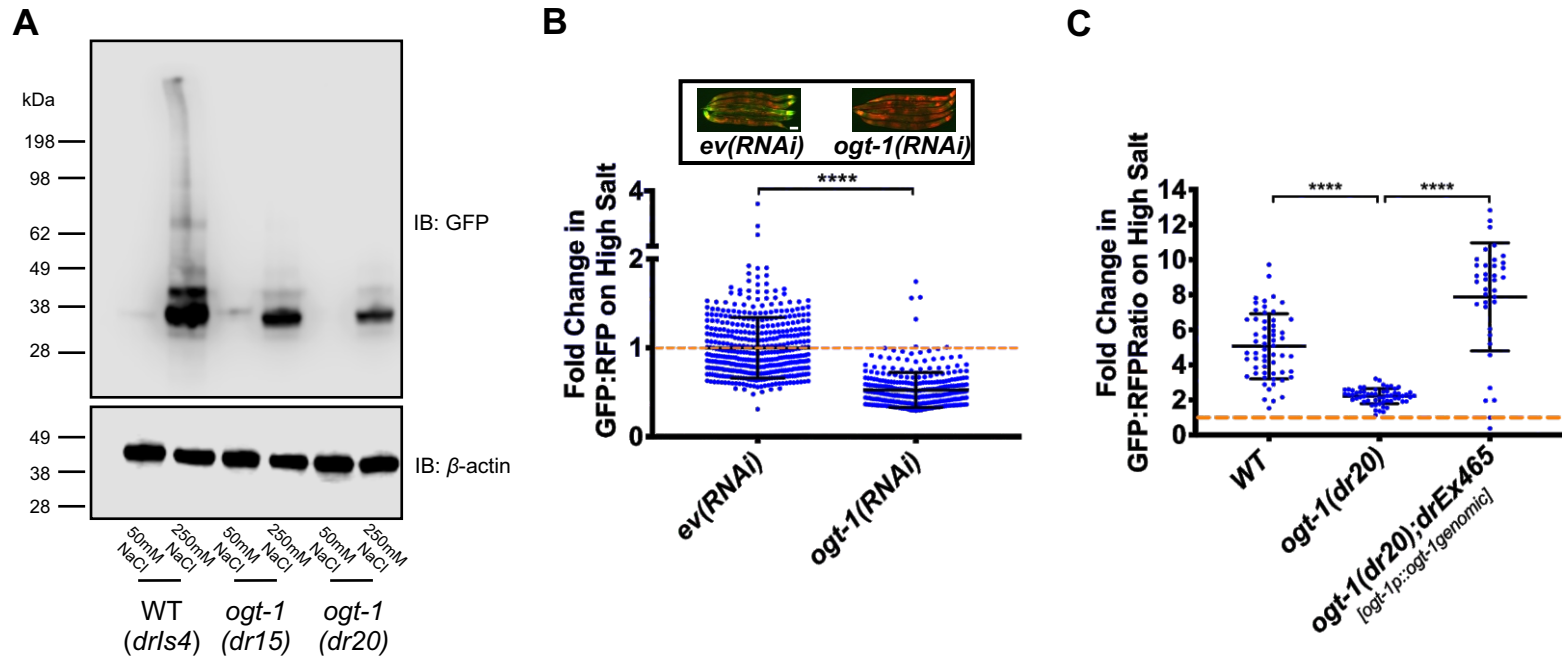


## Figure S2

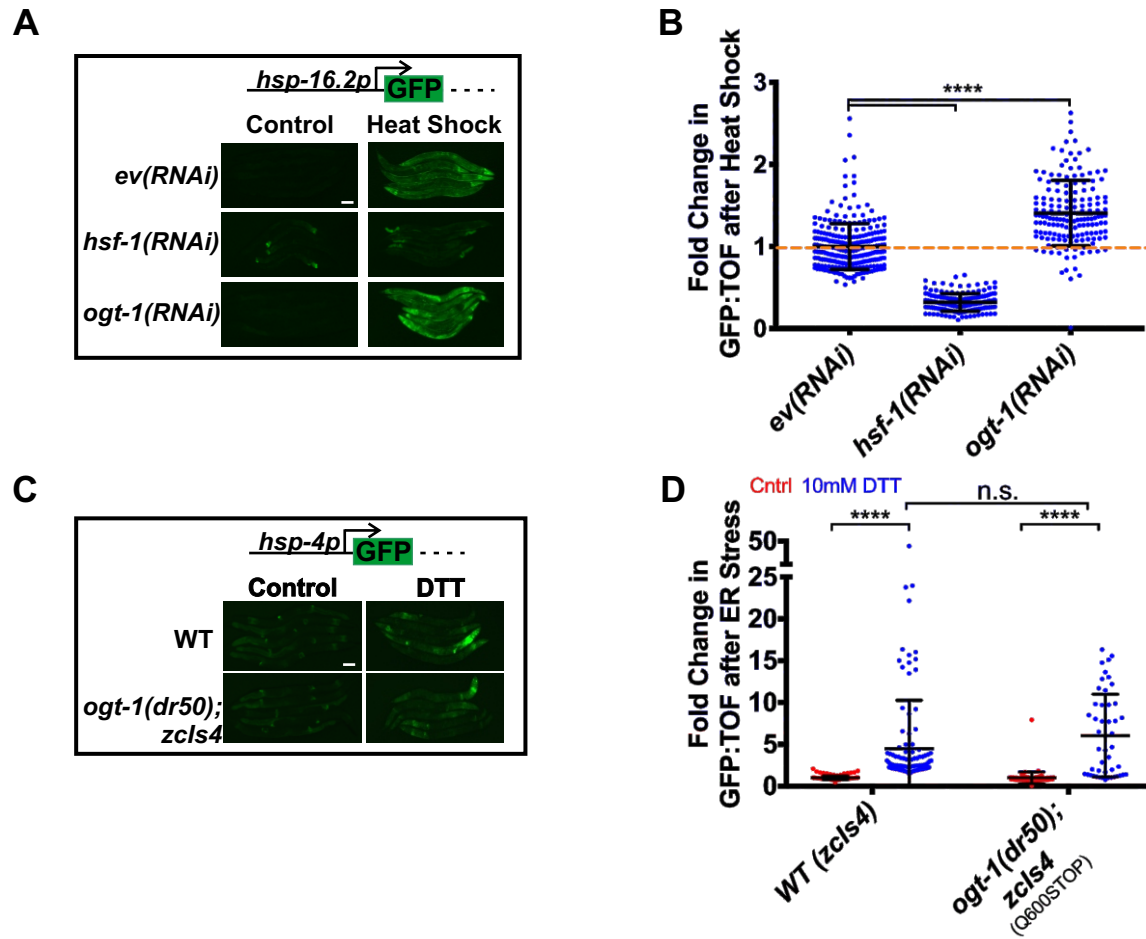
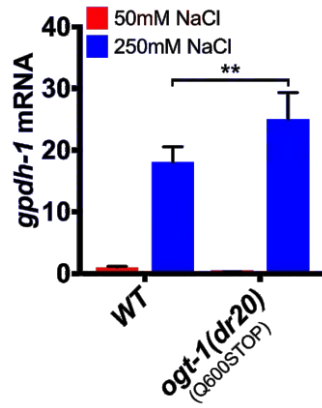


## Figure S3

**A**



**B**

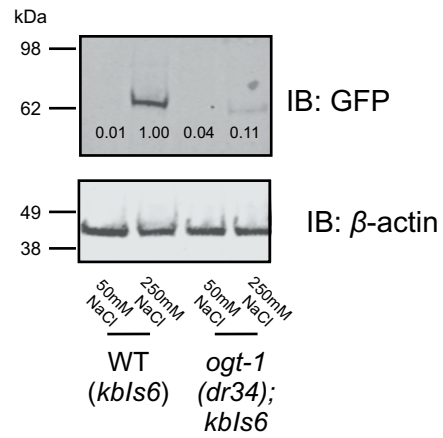


## Figure S4

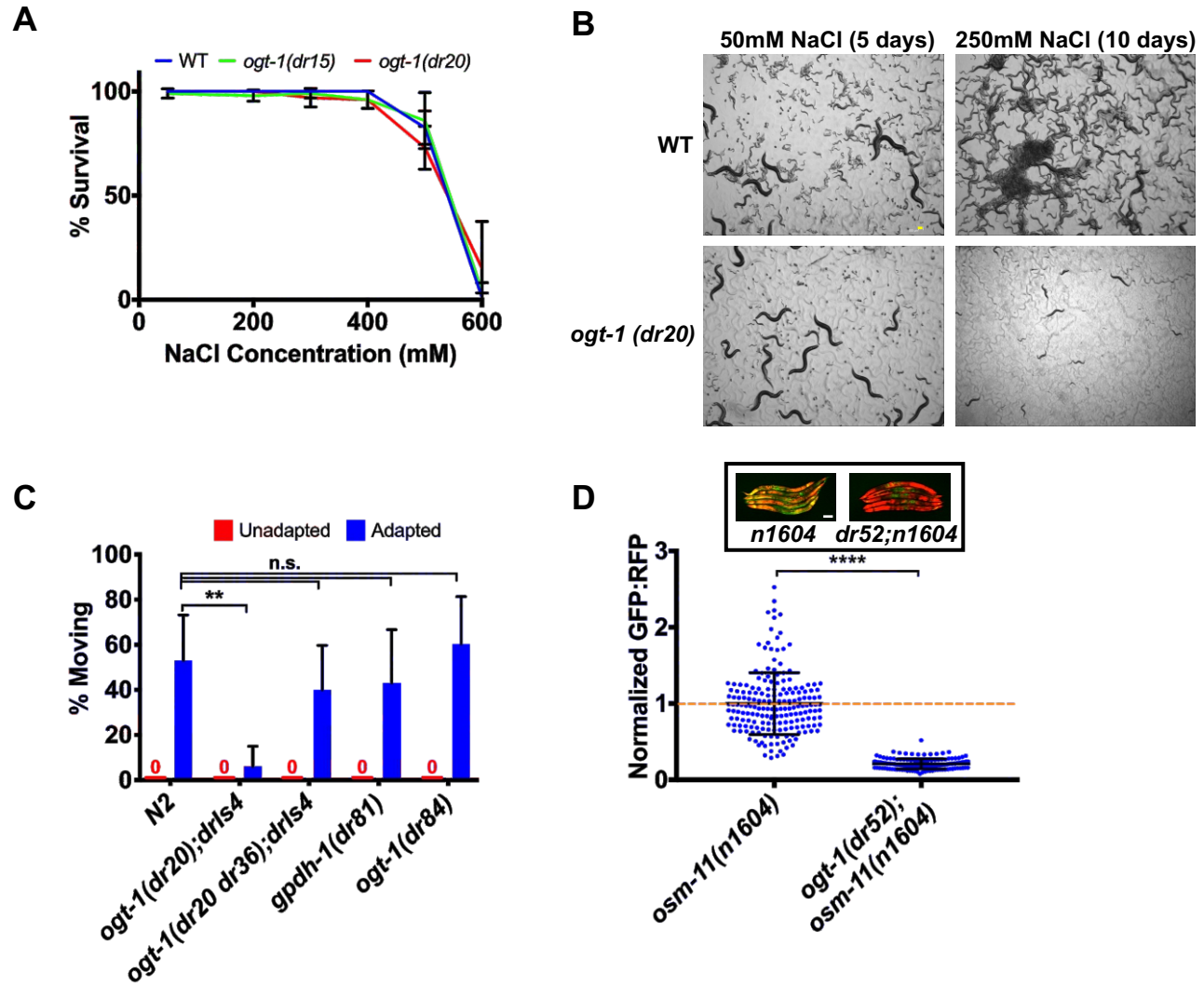


# Figure S5

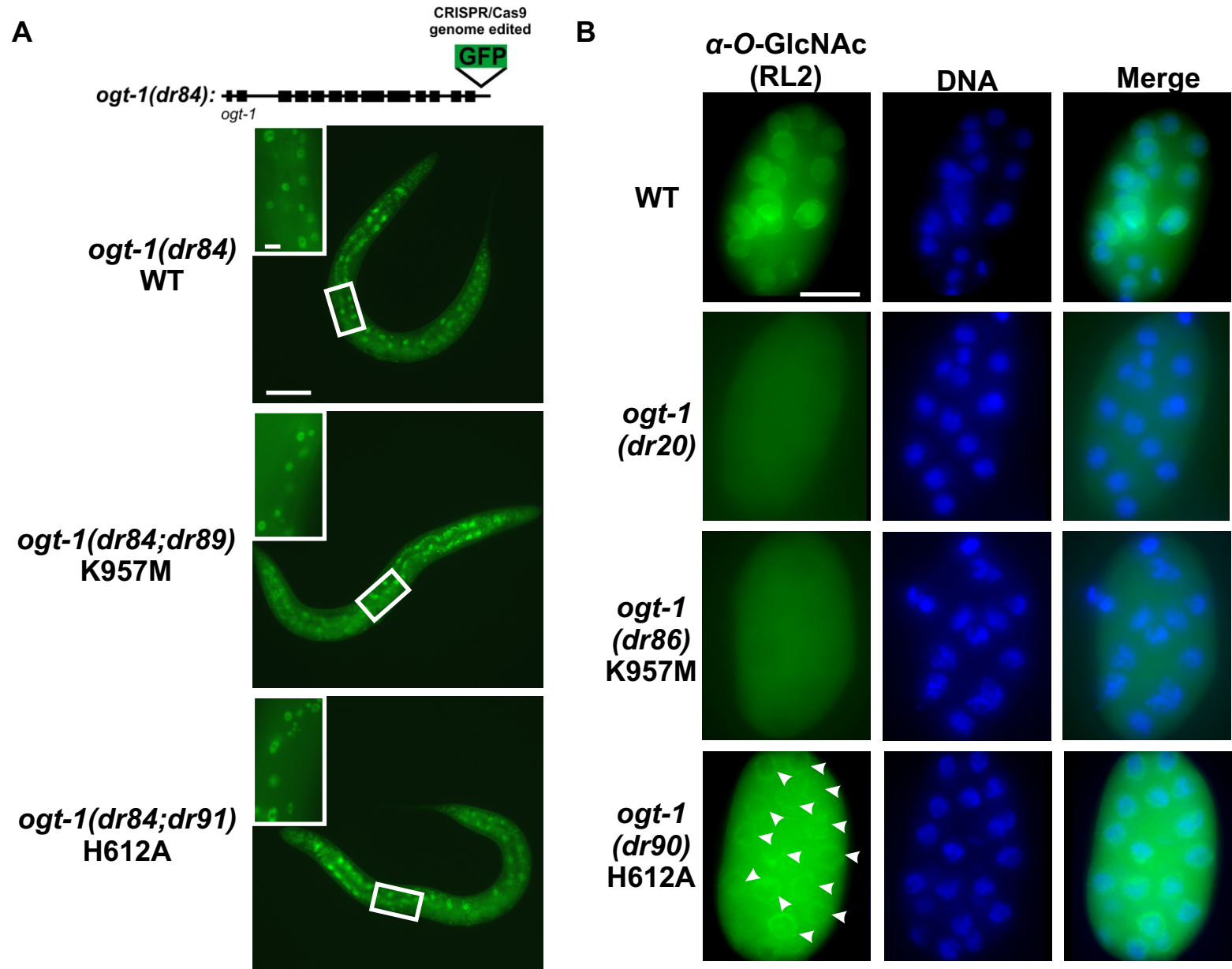
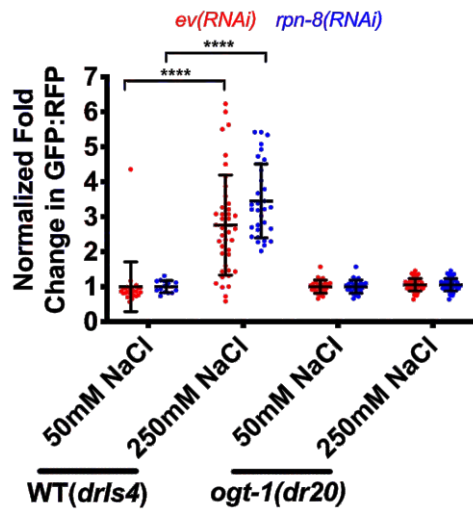


## Figure S6

**A**



**B**

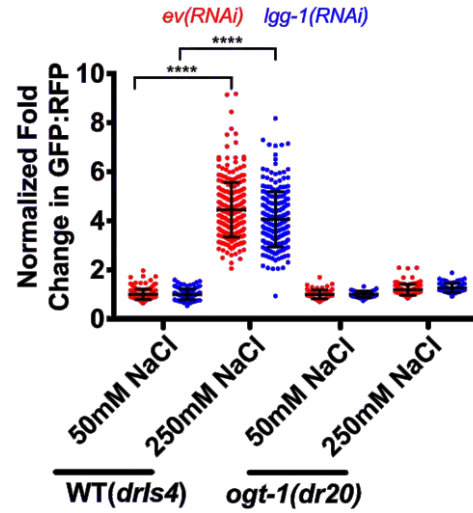


**Table S1**

Strain	Outcross	Number of Nio males from a cross of <i>ogt-1</i> x WT	Number of Nio among self progeny of <i>ogt-1/+</i>
<i>ogt-1(dr15)</i>	#1	0/30 (0%)	8/27 (30%)
	#2	0/20 (0%)	7/34 (21%)
	#3	0/15 (0%)	13/65 (20%)
<i>ogt-1(dr20)</i>	#1	0/20 (0%)	3/17 (18%)
	#2	*	7/34 (21%)
	#3	0/20 (0%)	17/70 (24%)

**Table S2**

		Mutant A			
Mutant B		<i>dr15</i>	<i>dr20</i>	<i>ok430</i>	<i>ok1474</i>
	<i>dr15</i>	8/18 (44%)	13/31 (42%)	6/12 (67%)	8/20 (40%)
	<i>dr20</i>		11/28 (39%)	9/32 (28%)	12/33 (36%)
	<i>ok430</i>			3/10 (30%)	13/27 (48%)
	<i>ok1474</i>				14/22 (64%)

Number of of animals with a Nio phenotype (no gfp induction on 250 mM NaCl) in the cross progeny of a ogt-1/+ male to an ogt-1/ogt-1 hermaphrodite  
 Complementation = 0%  
 Non-complementation = ~50%

**Table S3**

Strain	Number of unique non-synonymous SNPs	Number of unique non-synonymous INDELs
<i>ogt-1(dr15)</i>	377	72
<i>ogt-1(dr20)</i>	467	77
<i>ogt-1(dr20)</i> no backcrossing	596	85

**Table S4**

Strain	Genotype	Origin
OG119	<i>drls4</i> [ <i>gpdh-1p::GFP</i> ; <i>col-12p::dsRed2</i> ]	This study
VP223	<i>unc-119(ed3);kbls6</i> [ <i>gpdh-1p::gpdh-1-GFP</i> ]	This study
OG971	<i>ogt-1(dr15);drls4</i>	This study
OG969	<i>ogt-1(dr20);drls4</i>	This study
RB653	<i>ogt-1(ok430)</i>	<i>C. elegans</i> Gene Knockout Consortium (Oklahoma Medical Research Foundation, Oklahoma City)
OG1034	<i>ogt-1(ok430);drls4</i>	This study
RB1342	<i>ogt-1(ok1474)</i>	<i>C. elegans</i> Gene Knockout Consortium (Oklahoma Medical Research Foundation, Oklahoma City)
OG1035	<i>ogt-1(ok1474);drls4</i>	This study
OG1066	<i>ogt-1(dr20 dr36);drls4</i>	This study
OG1064	<i>ogt-1(dr34);unc-119(ed3);kbls6</i>	This study
OG1115	<i>gpdh-1(dr81)</i> [ <i>gpdh1::gfp</i> ]	This study
OG1123	<i>gpdh-1(dr81);ogt-1(dr84)</i>	This study
N2 Bristol	WT	<i>Caenorhabditis</i> Genetics Center
RB1373	<i>gpdh-1(ok1558)</i>	<i>C. elegans</i> Gene Knockout Consortium (Oklahoma Medical Research Foundation, Oklahoma City)
OG1048	<i>osm-8(dr9);unc-4(e120);drls4</i>	This study
OG1049	<i>osm-8(dr9); unc-4(e120);ogt-1(dr20);drls4</i>	This study
OG1111	<i>ogt-1(dr20);drls4;drEx468</i> [ <i>ogt-1p::ogt-1cDNA::ogt-1 3'utr</i> ; <i>rol-6(su1006)</i> ]	This study
OG1119	<i>ogt-1(dr20);drls4;drEx469</i> [ <i>dpy-7p::ogt-1cDNA::ogt-1 3'utr</i> ; <i>rol-6(su1006)</i> ]	This study
OG1120	<i>ogt-1(dr20);drls4;drEx470</i> [ <i>nhx-2p::ogt-1cDNA::ogt-1 3'utr</i> ; <i>rol-6(su1006)</i> ]	This study
OG1121	<i>ogt-1(dr20);drls4;drEx471</i> [ <i>myo-2p::ogt-1cDNA::ogt-1 3'utr</i> ; <i>rol-6(su1006)</i> ]	This study
OG1122	<i>ogt-1(dr20);drls4;drEx472</i> [ <i>rab-3p::ogt-1cDNA::ogt-1 3'utr</i> ; <i>rol-6(su1006)</i> ]	This study
OG1125	<i>ogt-1(dr20);drls4;drEx473</i> [ <i>ogt1p::humanOGTisoform1cDNA::ogt-1 3'utr</i> ; <i>rol-6(su1006)</i> ]	This study

OG1126	<i>ogt-1(dr20);drls4;drEx474</i> [ <i>ogt1p::humanOGTisoform1H498AcDNA::ogt-1 3'utr; rol-6(su1006)</i> ]	This study
OG1046	<i>ogt-1(dr20);drls4;drEx465</i> [ <i>ogt-1p::ogt-1genomic</i> ]	This study
TJ375	<i>gpls1</i> [ <i>hsp16.2p::GFP</i> ]	Link, C.D., Cypser, J.R., Johnson, C.J., and Johnson, T.E. (1999). Direct observation of stress response in <i>Caenorhabditis elegans</i> using a reporter transgene. <i>Cell Stress Chaperones</i> 4, 235-242.
SJ4005	<i>zcls4</i> [ <i>hsp4::GFP</i> ] V	Calfon, M., Zeng, H., Urano, F., Till, J.H., Hubbard, S.R., Harding, H.P., Clark, S.G., and Ron, D. (2002). IRE1 couples endoplasmic reticulum load to secretory capacity by processing the XBP-1 mRNA. <i>Nature</i> 415, 92-96.
OG1081	<i>ogt-1(dr50);zcls4</i>	This study
MT3643	<i>osm-11(n1604)</i>	Culotti, J.G., and Russell, R.L. (1978). Osmotic avoidance defective mutants of the nematode <i>Caenorhabditis elegans</i> . <i>Genetics</i> 90, 243-256.
OG1083	<i>ogt-1(dr52);osm-11(n1604)</i>	This study
OG1135	<i>ogt-1(dr86);drls4</i>	This study
OG1140	<i>ogt-1(dr90);drls4</i>	This study
OG1124	<i>ogt-1(dr84)</i> [ <i>ogt-1::GFP</i> ]	This study
OG1139	<i>ogt-1(dr84);ogt-1(dr89)</i>	This study
OG1141	<i>ogt-1(dr84);ogt-1(dr91)</i>	This study

**Table S5**

Primer name	sequence (5' – 3')	target	Purpose
OG1565	ACGGAAATTGGTACAAATTG TGG	<i>ogt-1(dr20)</i>	guide RNA for CRISPR/Cas9 conversion of the <i>dr20</i> SNP back to WT and the addition of the <i>dr20</i> SNP
OG1566	TCCCGGATGCATACTGTAATC	<i>ogt-1(dr20)</i>	inner nested <i>dr20</i> genotyping forward primer
OG1567	CCAAGCATTGGAACATGAACC	<i>ogt-1(dr20)</i>	inner nested <i>dr20</i> genotyping reverse primer
OG1568	GACAGCTCTCAAGCTGAAACCAG	<i>ogt-1(dr20)</i>	outer nested <i>dr20</i> genotyping outer nested forward primer
OG1569	GATCAGCGTGGATGAGTGGTGTC	<i>ogt-1(dr20)</i>	outer nested <i>dr20</i> genotyping reverse primer
OG1570	TATGATAAACGAGTACGGAAATTGGTACA AATTGT CGAAGATC AGCTTTGCAAGAAACGTCTTCCATCGGTT CATCCA	<i>ogt-1(dr20)</i>	ssODN repair template for CRISPR/Cas9 conversion of the <i>dr20</i> SNP back to WT
OG1571	TATGATAAACGAGTACGGAAATTGGTACA AATTGT CGAAGATT AGCTTTGCAAGAAACGTCTTCCATCGGTT CATCCA	<i>ogt-1</i>	ssODN repair template for CRISPR/Cas9 addition of the <i>dr20</i> SNP
OG1544	ACTATCACTTA ATCATACTC TGG	<i>gpdh-1</i>	guide RNA for CRISPR/Cas9 C-terminal addition of GFP
OG1546	ATGAGTAAAGGAGAAGAACT	pPD95.75	amplification of GFP for CRISPR/Cas9 C-terminal addition of GFP to <i>gpdh-1</i>
OG1547	TTTGTATAGTTCATCCATGC	pPD95.75	amplification of GFP for CRISPR/Cas9 C-terminal addition of GFP to <i>gpdh-1</i>
OG1548	CTGGAGATCAATGAAATCTCGGAAAAGTT CCCAATCTTCGCGTCAGTGCATAAGGTG TTCACCGGGCACACGGAGAGCAGGAG CTCTATGATTCCCTGAGAAACCATCCGGA ATACGACATGAGTAAAGGAGAAGAACT	pPD95.75	forward primer used to amplify GFP for CRISPR/Cas9 C-terminal <i>gpdh-1</i> insertion of GFP, includes 120 bp homology overhangs to site of insertion

OG1549	AAAATTGTACAATATACATACATAAATACC AGTAAAAAAGATTCAAAAACACGTGTTTT TTCTTTATATCCGCTAGATCCATTTCCAG CTCGTCAATAAAACACATAAACTATCAC TTATTTGTATAGTTCATCCATGC	pPD95.75	reverse primer used to amplify GFP for CRISPR/Cas9 C-terminal <i>gpdh-1</i> insertion of GFP, includes 120 bp homology overhangs to site of insertion
OG1708	TCAGTGCATAAGGTGTTACCG	<i>gpdh-1</i>	inner nested <i>gpdh-1::GFP</i> genotyping forward primer
OG1709	CTTTATATCCGCTAGATCCAT	<i>gpdh-1</i>	inner nested <i>gpdh-1::GFP</i> genotyping reverse primer
OG1710	CTCGGAAAAGTTCCCAATCTTC	<i>gpdh-1</i>	outer nested <i>gpdh-1::GFP</i> genotyping forward primer
OG1711	CCAGTAAAAAAGATTCAAAAACACG	<i>gpdh-1</i>	outer nested <i>gpdh-1::GFP</i> genotyping reverse primer
OG1664	GCTTGTGAATAGATTTTCGA AGG	<i>ogt-1</i>	guide RNA for CRISPR/Cas9 C-terminal addition of GFP
OG1665	ATATCACTAATAATACGGAAACGCCACAC GGCTTGATGAGTAAAGGAGAAGAAGCTTT TC	pPD95.75	5' Sp9-modified forward primer used to amplify GFP for CRISPR/Cas9 C-terminal <i>ogt-1</i> insertion of GFP, includes 35 bp homology overhangs to site of insertion
OG1666	GAAAATTATACAAAATATACAATTTTTTAA AAATCGTTCGAAAATCTATTCATTTGTATA GTTTCATCCATGCCATG	pPD95.75	5' Sp9-modified reverse primer used to amplify GFP for CRISPR/Cas9 C-terminal <i>ogt-1</i> insertion of GFP, includes 35 bp homology overhangs to site of insertion
OG1667	CTCACAGAGGTTCAACATTTTTTCC	<i>ogt-1</i>	outer nested <i>ogt-1::GFP</i> genotyping forward primer
OG1668	GAGCACTGAGGAGTAATACG	<i>ogt-1</i>	outer nested <i>ogt-1::GFP</i> genotyping reverse primer
OG1669	TTTCAGCTTGGCGAACATGCGT	<i>ogt-1</i>	inner nested <i>ogt-1::GFP</i> genotyping forward primer
OG1670	GGTTTCCAATATGGAAAATC	<i>ogt-1</i>	inner nested <i>ogt-1::GFP</i> genotyping reverse primer
OG1746	CTTGCCAGCATAACACAAGGATGC	<i>ogt-1</i>	outer nested OGT-1 H612A genotyping forward primer
OG1747	ATATGGCAGAAGCTATTCAAAG	<i>ogt-1</i>	inner nested OGT-1 H612A genotyping forward primer
OG1748	CCAAGCATTTGAACATGAACCTG	<i>ogt-1</i>	inner nested OGT-1 H612A genotyping reverse primer
OG1749	TCGATCAGCGTGGATGAGTGGTG	<i>ogt-1</i>	outer nested OGT-1 H612A genotyping reverse primer

OG1770	GGATAAAGCATACTGTGATG TGG	<i>ogt-1</i>	guide RNA for CRISPR/Cas9 conversion of the OGT-1 H612A SNP
OG1771	ATTGTGGAAGATCAGCTTTGCAAGAAAC GTCTTCCCTCAGTTCATCCAGCTCATTCT ATGCTCTACCCGCTTTACATGCGGCTC GGATTGCAATTGCTGCAAA	<i>ogt-1</i>	ssODN repair template for CRISPR/Cas9 conversion of the OGT-1 H612A SNP
OG1774	CAGAAGTAGTAAGTGGACCCAAC	<i>ogt-1</i>	outer nested OGT-1 K957M genotyping forward primer
OG1775	CCAATCAAGCAAATGATCATG	<i>ogt-1</i>	inner nested OGT-1 K957M genotyping forward primer
OG1776	AAGCCAAAGAATTGATTTCTGG	<i>ogt-1</i>	inner nested OGT-1 K957M genotyping reverse primer
OG1777	CCTCTCTCTACACAATACTTTCTG	<i>ogt-1</i>	outer nested OGT-1 K957M genotyping reverse primer
OG1772	ATCCACATGTCGAGAGTCGA TGG	<i>ogt-1</i>	guide RNA for CRISPR/Cas9 conversion of the OGT-1 K957M SNP

OG1773	atgctattgtgtttgcaattcaatcagctttacATGattgatc catctaccttagatatgtggattaaaattctcgagaatgttccg aaatcaattctttg	<i>ogt-1</i>	ssODN repair template for CRISPR/Cas9 conversion of the OGT-1 K957M SNP
OG1487	AAAGTGGGGGGGAGTTGAGAGT	<i>ogt-1</i>	forward primer for genomic <i>ogt-1</i>
OG1488	AAAATTTGTGTAGTGTTTT	<i>ogt-1</i>	reverse primer for genomic <i>ogt-1</i>
OG1649	TCTAAATACACTCACGTGACGCGTGGAT CCC	pPD61.125	forward primer for Gibson assembly
OG1650	CTCCCCCACTTTGGCTAGCCATGGAAC CGG	pPD61.125	Gibson assembly reverse primer
OG1651	CCATGGCTAGCCAAAGTGGGGGGAGTTG AG	<i>ogt-1</i> promoter	Gibson assembly forward primer for <i>ogt-1</i> promoter
OG1652	ATTGGGCTTCTCCATCGTCTAATCCATTC GATATAATTC	<i>ogt-1</i> promoter	Gibson assembly reverse primer for <i>ogt-1</i> promoter
OG1653	GGATTAGACGATGGAGAAGCCCAATTAC TTTCAGTC	<i>ogt-1</i> cDNA	Gibson assembly forward primer for <i>ogt-1</i> cDNA
OG1654	GAAAATCTATTCAAGCCGTGTGGCGT TTC	<i>ogt-1</i> cDNA	Gibson assembly reverse primer for <i>ogt-1</i> cDNA
OG1655	CCACACGGCTTGTGAATAGATTTTCGAA GGATTTTTAAAAAATTG	<i>ogt-1</i> 3'utr	Gibson assembly forward primer for <i>ogt-1</i> 3'utr
OG1656	CACGCGTCACGTGAGTGTATTTAGACGA GATTC	<i>ogt-1</i> 3'utr	Gibson assembly reverse primer for <i>ogt-1</i> 3'utr
OG1680	CAGATAAATGGAGAAGCCCAATTACTTTC AGTCG	<i>ogt-1p::ogt-1</i> cDNA:: <i>ogt-1</i> 3'utr	Gibson assembly forward primer for <i>dpy-7p</i> backbone
OG1681	TTGGTAGGGAGGCTAGCCATGGAACCGG	<i>ogt-1p::ogt-1</i> cDNA:: <i>ogt-1</i> 3'utr	Gibson assembly reverse primer for <i>dpy-7p</i> backbone
OG1682	ATGGCTAGCCTCCCTACCAATTGAAAATT C	<i>dpy-7</i> promoter	Gibson assembly forward primer for <i>dpy-7p</i>
OG1683	TGGGCTTCTCCATTTATCTGGAACAAAAT GTAAG	<i>dpy-7</i> promoter	Gibson assembly reverse primer for <i>dpy-7p</i>

OG1684	TTAAATCATGGAGAAGCCCAATTACTTTCAGTCG	<i>ogt-1p::ogt-1 cDNA::ogt-1 3'utr</i>	Gibson assembly forward primer for <i>nhx-2p</i> backbone
OG1685	TTTATTCAACGGCTAGCCATGGAACCGG	<i>ogt-1p::ogt-1 cDNA::ogt-1 3'utr</i>	Gibson assembly reverse primer for <i>nhx-2p</i> backbone
OG1686	ATGGCTAGCCGTTGAATAAACGCTTAGTC	<i>nhx-2 promoter</i>	Gibson assembly forward primer for <i>nhx-2p</i>
OG1687	TGGGCTTCTCCATGATTTAATCACTGAAAATTATTTTC	<i>nhx-2 promoter</i>	Gibson assembly reverse primer for <i>nhx-2p</i>
OG1692	CCATCTAGAAATGGAGAAGCCCAATTACTTTCAG	<i>ogt-1p::ogt-1 cDNA::ogt-1 3'utr</i>	Gibson assembly forward primer for <i>myo-3p</i> backbone
OG1693	cggccagaccGGCTAGCCATGGAACCGG	<i>ogt-1p::ogt-1 cDNA::ogt-1 3'utr</i>	Gibson assembly reverse primer for <i>myo-3p</i> backbone
OG1694	atggctagccGGTCTGGCCGCAAAAAGG	<i>myo-3p</i>	Gibson assembly forward primer for <i>myo-3p</i>
OG1695	GCTTCTCCATTTCTAGATGGATCTAGTGGTCG	<i>myo-3p</i>	Gibson assembly reverse primer for <i>myo-3p</i>
OG1696	GAAGAAGACCATGGAGAAGCCCAATTACTTTCAG	<i>ogt-1p::ogt-1 cDNA::ogt-1 3'utr</i>	Gibson assembly forward primer for <i>rab-3p</i> backbone
OG1697	AAGATGCACTGGCTAGCCATGGAACCGG	<i>ogt-1p::ogt-1 cDNA::ogt-1 3'utr</i>	Gibson assembly reverse primer for <i>rab-3p</i> backbone
OG1698	ATGGCTAGCCAGTGCATCTTCTTTTGAGAATTC	<i>rab-3p</i>	Gibson assembly forward primer for <i>rab-3p</i>
OG1699	GCTTCTCCATGGTCTTCTTCGTTTCCGC	<i>rab-3p</i>	Gibson assembly reverse primer for <i>rab-3p</i>
OG1700	TTAGACGATGGCGTCTTCCGTGGGCAAC	human <i>ogt</i> isoform 1	Gibson assembly forward primer for human <i>ogt-1</i>
OG1701	AATCTATTCATGCTGACTCAGTGACTTCAACAG	human <i>ogt</i> isoform1	Gibson assembly reverse primer for human <i>ogt-1</i>
OG1702	TGAGTCAGCATGAATAGATTTTTCGAAGGATTTTAAAAAATTG	<i>ogt-1p::ogt-1 cDNA::ogt-1 3'utr</i>	Gibson assembly forward primer for human <i>ogt</i> backbone
OG1703	CGGAAGACGCCATCGTCTAATCCATTTCG	<i>ogt-1p::ogt-1 cDNA::ogt-1 3'utr</i>	Gibson assembly reverse primer for human <i>ogt</i> backbone

OG535	CCCAATCCAAGAGAGGTATCCTT	<i>act-2</i>	qPCR forward primer
OG536	GAAGCTCGTTGTAGAAAGTGTGATG	<i>act-2</i>	qPCR reverse primer
OG592	TGCAGAGATTCCAGGAAACCAGG	<i>gpdh-1</i>	qPCR forward primer
OG593	CCCTTTTGTAGCTTGCCACGGAG	<i>gpdh-1</i>	qPCR reverse primer
OG876	CCATTGAAGAGGTAGAAATGC	<i>hmit-1.1</i>	qPCR forward primer
OG877	TGTACTTCATTGTGTTGTCC	<i>hmit-1.1</i>	qPCR reverse primer
OG878	GAGGATATGGAAGAGGATATGG	<i>nlp-29</i>	qPCR forward primer
OG879	GTATCCTCCGTACATTCCAC	<i>nlp-29</i>	qPCR reverse primer
OG1342	TACCTGTTCCATGGCCAACACTTGTC	<i>GFP</i>	qPCR forward primer
OG1343	CTTTCCTGTACATAACCTTCGGGC	<i>GFP</i>	qPCR reverse primer

**Table S6**

Strain name	Genotype	Origin
<i>E. coli</i> OP50		Caenorhabditis Genetics Center
<i>E. coli</i> HT115		Caenorhabditis Genetics Center

**Table S7**

<b>Reagent</b>	<b>Source</b>	<b>Catalog #</b>
Anti-GFP primary antibody produced in mouse (clones 7.1 and 13.1)	Roche	11814460001
Monoclonal Anti- $\beta$ -Actin primary antibody produced in mouse (clone AC-15)	Sigma Life Sciences	A1978
Mouse Anti-O-Linked N-Acetylglucosamine (O-GlcNAc) monoclonal antibody (RL2)	Thermo Fisher Scientific Invitrogen	MA1-072
Anti-mouse horseradish peroxidase (HRP) – linked secondary antibody	Cell Signaling Technologies	7076S
Goat anti-Mouse IgG (H+L) Cross-Absorbed Secondary Antibody, DyLight 800	Thermo Fisher Scientific	SA5-10176
Goat anti-Mouse IgG, IgM (H+L) Secondary Antibody, Alexa Fluor 488	Thermo Fisher Scientific	A-10680
<i>Mbo</i> I Restriction Endonuclease	New England BioLabs	R0147S
<i>Dde</i> I Restriction Endonuclease	New England BioLabs	R0152S
Alt-R S.p. Cas9 Nuclease V3	Integrated DNA Technologies (IDT)	1081058

**Table S8**

<b>Assay</b>	<b>Source</b>	<b>Catalog #</b>
RNeasy Mini Kit	Qiagen	74106
SuperScript VILO Master Mix	Thermo Fisher Scientific	11755050
SYBER Green PCR Master Mix	Thermo Fisher Scientific	4344463
NuPAGE LDS Sample Buffer (4X)	Thermo Fisher Scientific	NP0007
NuPAGE Sample Reducing Agent (10X)	Thermo Fisher Scientific	NP0009
Blot 8% Bis-Tris Plus	Thermo Fisher Scientific	NW00082BOX
Blot 4-12% Bis-Tris Plus	Thermo Fisher Scientific	NW04122BOX
iBlot 2 NC Regular Stacks	Thermo Fisher Scientific	IB23001
iBind Cards	Thermo Fisher Scientific	SLF1010
iBind Solution Kit	Thermo Fisher Scientific	SLF1020
iBind Flex Fluorescent Detection (FD) Solution Kit	Thermo Fisher Scientific	SLF2019
Gentra Puregene Tissue Kit	Qiagen	158667